AD-A045 321 IOWA UNIV IOWA CITY DEPT OF PHYSICS AND ASTRONOMY F/G 20/9

PLASMA WAVES IN THE POLAR CUSP: OBSERVATIONS FROM HAWKEYE 1.(U)

JUL 77 D A GURNETT, L A FRANK N00014-76-C-0016

UNCLASSIFIED U. OF IOWA-77-21 NL

| OF |

AD A045321

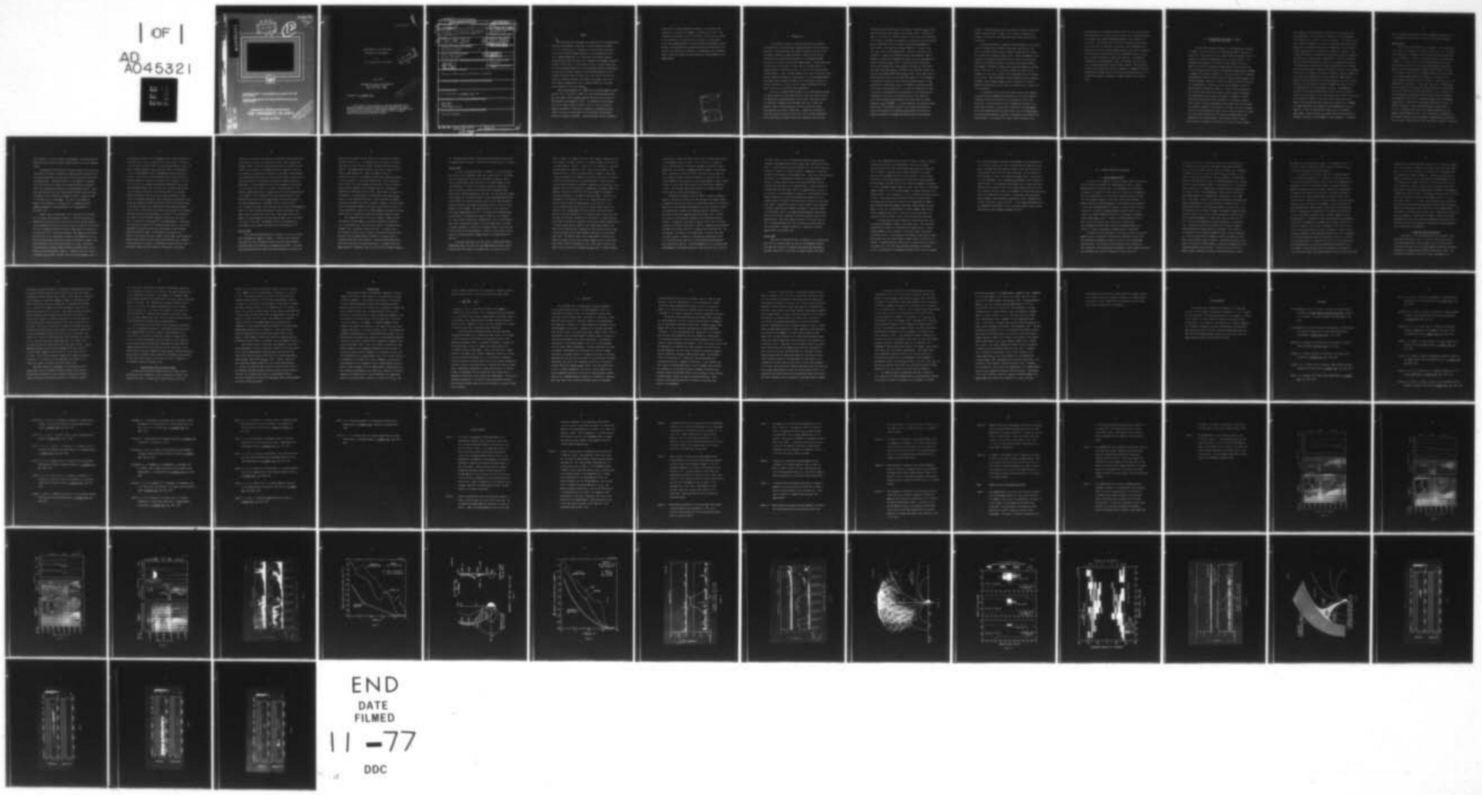

END

DATE FILMED

11-77

DDC

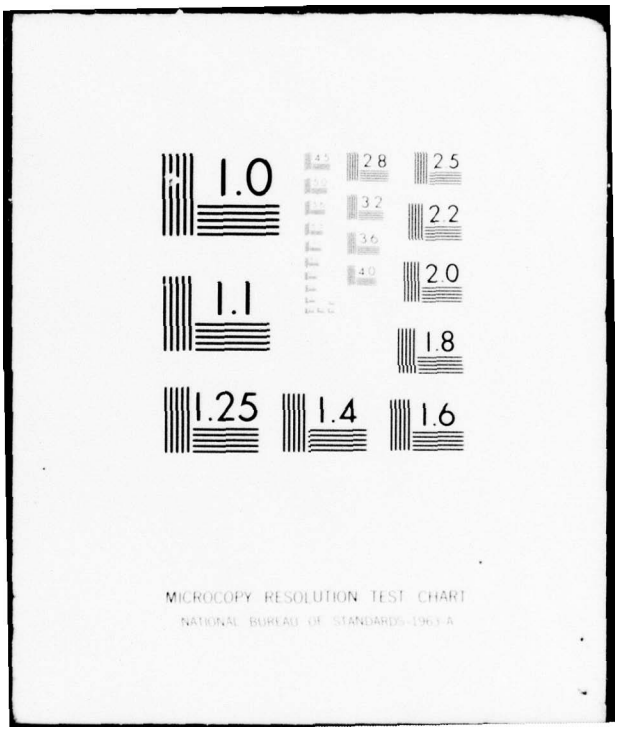
1.0
1.1
1.25
1.4
1.6
2.8
2.5
3.2
2.2
3.6
2.0
4.0
1.8
MICROCOPY RESOLUTION TEST CHART
NATIONAL BUREAU OF STANDARDS-1963-A

U. of Iowa 77-21

12

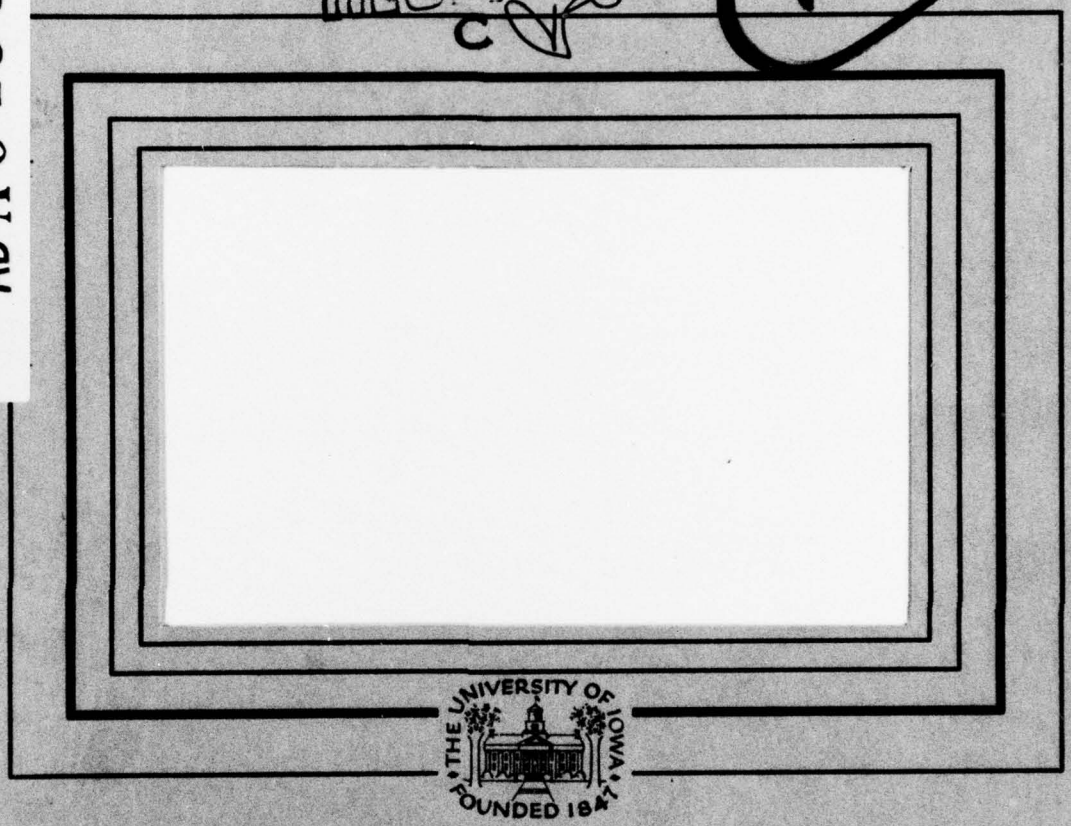

Department of Physics and Astronomy
THE UNIVERSITY OF IOWA
Iowa City, Iowa 52242

U. of Iowa 77-21

Plasma Waves in the Polar Cusp: Observations from Hawkeye 1

by

D. A. Gurnett and L. A. Frank

July, 1977

Department of Physics and Astronomy
The University of Iowa
Iowa City, Iowa 52242

Submitted to J. Geophys. Res.

The research at the University of Iowa was supported by the National Aeronautics and Space Administration through Grants NGL-16-001-002 and NGL-16-001-043, through Contracts NAS1-11257 and NAS1-13129 with Langley Research Center, and by the U. S. Office of Naval Research through Contract N00014-76-C-0016.

UNCLASSIFIED
SECURITY CLASSIFICATION OF THIS PAGE (When Data Entered)

REPORT DOCUMENTATION PAGE

READ INSTRUCTIONS BEFORE COMPLETING FORM

1. REPORT NUMBER: U. of Iowa-77-21	2. GOVT ACCESSION NO.
3. RECIPIENT'S CATALOG NUMBER: (9) Progress rept.,	
4. TITLE (and Subtitle): Plasma Waves in the Polar Cusp: Observations from Hawkeye 1	5. TYPE OF REPORT & PERIOD COVERED: Progress, July 1977
	6. PERFORMING ORG. REPORT NUMBER
7. AUTHOR(s): D. A. Gurnett and L. A. Frank	8. CONTRACT OR GRANT NUMBER(s): N00014-76-C-0016, NAS1-11257
9. PERFORMING ORGANIZATION NAME AND ADDRESS: Department of Physics and Astronomy, The University of Iowa, Iowa City, IA 52242	10. PROGRAM ELEMENT, PROJECT, TASK AREA & WORK UNIT NUMBERS
11. CONTROLLING OFFICE NAME AND ADDRESS: Office of Naval Research, Arlington, VA 22217	12. REPORT DATE: July 1977
	13. NUMBER OF PAGES: 69
14. MONITORING AGENCY NAME & ADDRESS(if different from Controlling Office): (12) 71 p.	15. SECURITY CLASS. (of this report): UNCLASSIFIED
	15a. DECLASSIFICATION/DOWNGRADING SCHEDULE

16. DISTRIBUTION STATEMENT (of this Report)

Approved for public release; distribution is unlimited.

17. DISTRIBUTION STATEMENT (of the abstract entered in Block 20, if different from Report)

18. SUPPLEMENTARY NOTES

To be published in J. Geophys. Res., 1977.

19. KEY WORDS (Continue on reverse side if necessary and identify by block number)

Plasma Waves
Polar Cusp
ULF-ELF Magnetic Noise

20. ABSTRACT (Continue on reverse side if necessary and identify by block number)

[See page following.]

DD FORM 1 JAN 73 1473 EDITION OF 1 NOV 65 IS OBSOLETE
S/N 0102-014-6601

UNCLASSIFIED
SECURITY CLASSIFICATION OF THIS PAGE (When Data Entered)

188 460

ABSTRACT

In this paper we investigate the characteristics of plasma waves observed by the Hawkeye 1 spacecraft in the vicinity of the polar cusp. The primary types of plasma waves associated with the polar cusp are (1) a band of ULF-ELF magnetic noise extending from a few Hz to several hundred Hz, (2) a broad-band electrostatic emission extending from a few Hz to about 30 to 100 kHz, with maximum intensities at about 10 to 50 Hz, (3) electrostatic electron cyclotron waves near the electron gyrofrequency and (4) whistler-mode auroral hiss emissions. Of these various types of waves, only the ULF-ELF magnetic noise is uniquely associated with the cusp in the sense that the noise can be used as a reliable indicator of the polar cusp region. All of the other types of plasma waves occur in regions adjacent to the polar cusp as well as in the cusp itself.

Spectrum measurements often show that the ULF-ELF magnetic noise extends up to, but does not exceed, the local electron gyrofrequency, f_g. This upper cutoff strongly suggests that the noise consists of whistler-mode electromagnetic waves. The mechanism for generating these waves remains highly uncertain, however, since the electron angular distribution in the cusp is usually not sufficiently anisotropic to account for these waves by the well known whistler-mode cyclotron resonance instability. Other mechanisms, such as turbulence

generated by the Kelvin-Helmholtz instability or by a drift wave instability, have also been suggested to generate this noise. The broad-band electrostatic noise is believed to be caused by a current-driven electrostatic instability (ion-cyclotron or ion-acoustic) of the type widely believed to occur in auroral field-aligned current systems. The mechanisms for generating electron cyclotron waves and auroral hiss emissions are believed to be reasonably well understood, based on previous studies of these emissions in other regions of the magnetosphere.

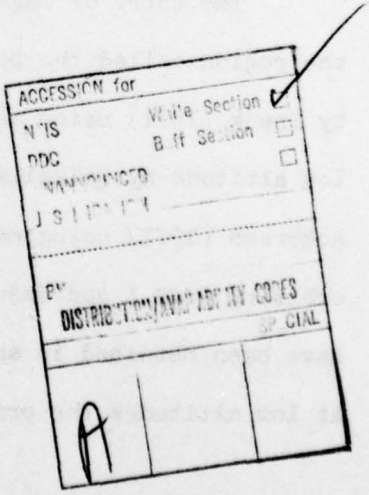

I. INTRODUCTION

In this paper we present a detailed study and investigation of plasma waves in the polar cusp using measurements from the Hawkeye 1 spacecraft. This spacecraft has a highly eccentric polar orbit with the apogee located at a radial distance of about 20.5 R_e over the north pole and is specifically designed for investigating plasma processes in the polar cusp and polar magnetosphere. The data presented in this study cover a period of about two and one-half years of in-flight operation, starting from launch on June 3, 1974, and extending through January 1, 1977. Secular changes in the orbit during this period provide excellent coverage of a broad region of the polar magnetosphere, with polar cusp crossings occurring over a wide range of radial distances, from about 5 to 10 R_e over the northern hemisphere and from about 1.1 to 2.0 R_e over the southern hemisphere.

The entry of magnetosheath plasma into the magnetosphere through the region called the polar cusp was first reported at high altitudes by Frank [1971] using measurements from the IMP 5 spacecraft, and at low altitude by Heikkila and Winningham [1971] and by Frank and Ackerson [1971] using measurements from the low-altitude polar-orbiting ISIS 1 and Injun 5 spacecraft. Plasma wave observations have been obtained in and near the polar cusp by several spacecraft. At low altitudes the primary plasma wave phenomenon which has been

associated with the polar cusp is auroral hiss [Laaspere et al., 1971; Gurnett and Frank, 1972; Laaspere and Hoffman, 1976]. At high altitudes, in the region of primary interest for the entry and acceleration of the polar cusp plasma, the plasma wave observations are more limited. Only two spacecraft, OGO 5 and HEOS 2, have provided plasma wave measurements in the polar cusp at high altitudes. Of these, only OGO 5 has electric field measurements. The OGO 5 observations are limited to a single event obtained during a large magnetic storm on November 1, 1968, which displaced the polar cusp to an abnormally low latitude [Russell et al., 1971]. During this event intense wave levels were observed over a broad range of frequencies, both within the polar cusp [Scarf et al., 1972] and in the interface between the cusp and the magnetosheath [Scarf et al., 1974]. The primary types of waves detected by OGO 5 in the polar cusp consist of (1) ULF magnetic fluctuations at frequencies below the proton gyrofrequency, $f \leq f_g^+$, identified as ion-cyclotron waves, (2) impulsive broad-band electric field bursts, with frequencies of ~ 3.0 kHz and intensities as large as 33 mV m^{-1}, associated with steep gradients in the plasma density and magnetic field, and (3) broad-band electric field emissions with a low frequency cutoff near the local lower hybrid resonance frequency, $f_{LHR} \simeq \sqrt{f_g^- f_g^+}$. In a later analysis, the impulsive broad-band electric field bursts observed in the polar cusp during this event were interpreted by Fredricks et al. [1973] as being due to either ion-acoustic or Buneman mode waves driven by field-aligned

currents. Fredricks et al. [1973] also presented evidence that field-aligned potential drops as large as 2 kV could be produced by the anomalous resistivities associated with these large electric field intensities.

Further measurements of magnetic field fluctuations in the polar cusp were obtained from the HEOS 2 spacecraft, which has an orbit chosen to provide repeated passes through the high altitude regions of the polar cusp [D'Angelo et al., 1974]. Intense ULF magnetic field turbulence, extending from frequencies below 20 Hz to greater than 236 Hz, was frequently detected in the polar cusp region by HEOS 2. This magnetic turbulence typically had a power law amplitude spectrum, $A \propto f^{-n}$, with $n \simeq 1.5 - 2.0$, and was usually most intense at the boundaries of the cusp, in regions with large gradients in the plasma flow velocity. These ULF magnetic field fluctuations were interpreted [D'Angelo, 1973; D'Angelo et al., 1974] as being due to a Kelvin-Helmholtz instability excited at the cusp boundaries by a shear in the ion flow velocity.

In comparison with the OGO 5 and HEOS 2 results, the Hawkeye 1 spacecraft provides plasma wave measurements over a broader range of frequencies with better electric field coverage and better time resolution. The most prominent type of plasma wave detected in the polar cusp by Hawkeye 1 consists of a broad band of ULF-ELF magnetic field noise extending from frequencies below 1 Hz up to approximately the electron gyrofrequency, f_g^-, which is typically a few hundred Hz at high altitudes. The evidence of an upper cutoff frequency to the

ULF-ELF magnetic noise spectrum suggests that this noise may consist of whistler-mode waves. Electric field intensities are surprisingly small in the polar cusp, seldom exceeding broad-band field strengths of 1 to 5 mV m^{-1}. The primary types of electric field emissions detected in the cusp are (1) broad-band electrostatic noise extending from a few Hz up to near the electron plasma frequency, f_p^-, which is typically 30 to 100 kHz, (2) electrostatic electron cyclotron waves at $f \simeq f_g^-$, and (3) quasi-electrostatic auroral hiss emissions. The Hawkeye 1 observations of ULF-ELF magnetic noise in the polar cusp are found to be in substantial agreement with the HEOS 2 results. The much lower electric field intensities detected by Hawkeye 1, compared to the OGO 5 observations, indicate that the storm time event detected by OGO 5 is unusual and probably not typical of normal conditions in the polar cusp.

II. SOME REPRESENTATIVE HAWKEYE 1 PASSES THROUGH THE POLAR CUSP

To illustrate the general features of the plasma waves observed by Hawkeye 1 we first discuss four representative passes through the polar cusp. These passes were all selected near the magnetic local noon meridian to eliminate complications due to local time effects. The plasma wave and magnetic field data for these passes are shown in Figures 1-4 and the corresponding charged particle measurements from the low-energy proton and electron differential energy analyzer (LEPEDEA) on Hawkeye 1 are shown in Plates 1-4. Since the details of the Hawkeye 1 instruments have been described in previous reports [Kurth et al., 1975; Gurnett and Frank, 1976] only a few brief comments are made concerning the instrumentation. Both the electric and the magnetic fields of plasma waves are detected by Hawkeye 1. Electric field measurements are obtained from a 42.45 meter electric dipole antenna and magnetic field measurements are provided by a search coil magnetic antenna. Electric field intensities are determined in 16 frequency channels, from 1.78 Hz to 178 kHz, and magnetic field intensities are determined in 8 frequency channels, from 1.78 Hz to 5.62 kHz. The field strengths for each of these channels are shown in the bottom two panels of Figures 1-4. The intensity scale for each channel is proportional to the logarithm of the field strength, with a range of 100 db from the base line of one channel to the base line of the next higher channel.

Static magnetic field measurements are provided by a tri-axial flux gate magnetometer. The top panels of Figures 1-4 give the magnetic field magnitude and direction in polar coordinates. The angle θ^B is the angle between the magnetic field and the spacecraft spin axis and the angle φ^B is the azimuthal direction of the magnetic field projected in a plane perpendicular to the spin axis. Because of a failure in the attitude determination system about 3 months after launch, the magnetic field direction usually cannot be determined in inertial coordinates. When the attitude determination system is not operating the angle φ^B is computed using an approximate average spin period and an arbitrary initial reference angle. Although the absolute direction of the magnetic field cannot be determined under these conditions, relative changes and short time scale fluctuations are easily detected. Measurements of positive ions and electrons in the energy range $50\ eV \leq E \leq 40\ keV$ are provided by an electrostatic analyzer (LEPEDEA) which has a field of view perpendicular to the spacecraft spin axis. The LEPEDEA also includes a thin-windowed Geiger-Mueller (GM) tube which responds to electrons with energies $E > 45$ keV and protons with energies $E > 650$ keV. The two panels of Plates 1-4 are color coded energy-time spectrograms of the electron and proton intensities detected by the LEPEDEA. The small panel above each energy-time spectrogram gives the pitch angle (0° to 180°) of the particles shown in the corresponding spectrogram. Since the polar cusp, particularly at low altitudes, is strongly controlled by the geomagnetic field, geomagnetic coordinates

are used throughout this paper. MLT is the magnetic local time, λ_m is the magnetic latitude and R is the geocentric radial distance.

Day 172, 1976

The first representative pass, in Figure 1, is an inbound pass near local noon at a magnetic local time of about 13.7 hr. The spacecraft trajectory in a magnetic meridian plane through the spacecraft (R, λ_m coordinates) is shown by the small sketch in the center panel of Figure 1. As can be seen, the spacecraft approaches the earth from a very high latitude in the polar cap, gradually decreasing in latitude with decreasing radial distance from the earth. At a magnetic latitude of about 65° and a radial distance of 6.2 R_e a region of high density magnetosheath-like plasma is encountered. This region, from about 1422 to 1434 UT in Plate 1, is the polar cusp. The maximum proton intensities in this region occur in the energy range from about 500 eV to 2 keV, and the proton densities and temperatures are about 45 cm^{-3} and 9 x 10^6°K, respectively. These parameters are in good quantitative agreement with the previous polar cusp plasma measurements by Frank [1971], Rosenbauer et al. [1975] and Paschmann et al. [1976]. Inspection of the angular distribution of proton intensities in plate 1 shows a distinct maximum at pitch angles of about 0°, indicating a directed flow of plasma downward along the magnetic field toward the earth. These observations, together with the spatial location, provide substantial evidence that this region is the polar cusp. After the polar cusp crossing the intensity of electrons

with energies, $E \geq 5$ keV, increases substantially, indicating that the spacecraft has entered the stable trapping region of the outer magnetosphere.

The magnetic field variations during this pass, shown in the top three panels of Figure 1, indicate a relatively smooth transition from the nearly radial field over the polar cap to the dipolar field within the magnetosphere. Small perturbations in the magnetic field magnitude and direction are evident as the spacecraft passes through the polar cusp, indicating the presence of field-aligned currents. Since the cusp crossing occurs at an intermediate altitude between the magnetosheath and the ionosphere the magnetic field is relatively large in the polar cusp, $B \simeq 200$ gammas. The ratio of the plasma to magnetic field pressure in the polar cusp is estimated from the LEPEDEA and magnetic field measurements to be approximately $\beta = 8\pi\, nkT/B^2 \simeq 0.6$.

Several types of plasma waves can be identified in association with the polar cusp crossings in Figure 1. The most prominent wave phenomena associated with the cusp are (1) a band of ULF-ELF magnetic noise extending from below 1.78 Hz up to about 1.78 kHz and (2) numerous bursts of broad-band electric field noise extending up to frequencies as high as 56.2 kHz. Other wave phenomena, also apparently associated with the cusp but not necessarily confined to the immediate vicinity, are the whistler-mode auroral hiss emissions indicated in Figure 1 and the electrostatic electron cyclotron waves at $f \simeq f_g^-$. The auroral hiss and electron cyclotron waves are shown in greater detail by the frequency-time spectrogram in Figure 5. Comparison with the results of D'Angelo *et al.* [1974] indicates that the ULF-ELF magnetic noise is

essentially identical to the ULF magnetic noise detected by HEOS 2 in the polar cusp. Since the electric field noise bursts in the cusp extend to frequencies well above the electron gyrofrequency ($f_g^- \simeq 5.6$ kHz) it seems reasonably certain that this noise is electrostatic, since no electromagnetic mode of propagation occurs at these frequencies. The electric field spectrum of this noise, at a time of maximum intensity, is shown by the dashed line in Figure 6. As can be seen, this noise extends with detectable amplitudes over a very broad frequency range, from less than 1 Hz to greater than 100 kHz. The low frequency component of this noise, which is not clearly evident in Figure 1, can be seen more clearly in Figure 5. This noise is essentially identical to the "broad-band electrostatic noise" previously reported by Gurnett and Frank [1977] at other local times on the auroral field lines. Although the broad-band electrostatic noise is quite evident during this polar cusp crossing, the integrated broad-band electric field strength, $E \simeq 4.8$ mV m^{-1}, is substantially less than the field strengths typically observed for this type of noise in the local evening regions of the magnetosphere. The auroral hiss emissions in Figure 5 are identified on the basis of their close similarity to previous auroral hiss observations at low altitudes [Gurnett and Frank, 1972]. As indicated by the dashed line in Figure 5, the auroral hiss has a sharply defined upper cutoff frequency which closely tracks the local electron gyrofrequency, f_g^-. Although the auroral hiss is observed a considerable distance from the cusp, it seems most likely that this radiation is produced by low-energy

electrons in the polar cusp since this relationship has been previously established at low altitudes [Gurnett and Frank, 1972; Laaspere and Hoffman, 1976]. Since the whistler-mode auroral hiss emissions cannot reverse their direction of propagation along the magnetic field once the radiation is generated, the decrease in the upper cutoff frequency with decreasing radial distance from the earth provides strong evidence that these emissions are generated substantial distances below the spacecraft. A representative electric field spectrum of the auroral hiss is shown by the solid line in Figure 6 at about 1345 UT. The sporadic narrow-band emission slightly above the electron gyrofrequency f_g^- in Figure 5 is an electrostatic electron cyclotron wave, of the type first observed by Kennel et al. [1970] in the inner regions of the earth's magnetosphere. Although electron cyclotron waves are observed in the polar cusp, this same type of local (non-propagating) emission is also observed with sporadic intensity variations over a large region on either side of the cusp. Thus, these waves do not appear to be particularly associated with the polar cusp, even though they occur in the cusp. The maximum electric field amplitude of these waves is quite small, typically only a few hundred $\mu V\ m^{-1}$.

Day 174, 1976

The second representative pass, in Figure 2, occurs on the next orbit following the example in Figure 1. This pass was selected to illustrate the close similarities which are often observed between successive polar cusp crossings at intermediate altitudes. The spacecraft again approaches the earth from high latitudes in the polar cap

and crosses the polar cusp near local noon at a geocentric radial distance of about 6 R_e. The LEPEDEA data for this pass, in Plate 2, shows that the polar cusp is broader, extending from about 1712 to 1800 UT. The maximum proton density in this case is about 40 cm^{-3} and β is approximately 0.2. Again the magnetic field is relatively strong, $B \simeq 150$ gammas, with only very small perturbations in the cusp region. On the high latitude side of the cusp, before about 1748 UT, the proton angular distributions, evident in Plate 2, show a distinct maximum at pitch angles near 180°, indicating a plasma flow outward away from the earth. This region is believed to correspond to the plasma mantle, as discussed by Rosenbauer et al. [1975]. As the spacecraft proceeds to lower latitudes the angular distribution becomes more nearly isotropic. Finally, in a narrow region on the low latitude boundary of the polar cusp, at about 1759 UT, a distinct maximum is evident in the proton angular distribution at pitch angles near 0°, indicating a plasma flow downward toward the earth.

The plasma wave data for the pass in Figure 2 again show the occurrence of ULF-ELF magnetic noise and broad-band electrostatic noise in the polar cusp, with some of the bursts of broad-band electrostatic noise extending as high as 100 kHz. No auroral hiss or electrostatic electron cyclotron waves are detected during this pass. The entry into the magnetosphere is marked by an abrupt onset of continuum radiation at about 1800 UT. Gurnett and Shaw [1973] have previously shown that the continuum radiation is trapped within the magnetosphere at frequencies below the local electron plasma frequency,

f_p^-. The approximate electron plasma frequency variation at the polar cusp/magnetosphere boundary is indicated by the dashed lines in Figure 2.

Day 186, 1974

The third representative pass, in Figure 3, is an inbound pass near local noon at a magnetic local time of about 12.5 hr. This pass, which occurs about two years before the passes in Figures 1 and 2, is at a substantially lower latitude due to secular changes in the orbit parameters. Because of the lower latitude the spacecraft in this case enters the polar cusp directly from the magnetosheath, without first passing through the polar cap. The low latitude boundary of the polar cusp is clearly evident in both the plasma and wave data at about 2255 UT. Plate 3 shows that prior to this time substantial fluxes of protons with energies from about 200 eV to 2 keV are being detected by the LEPEDEA. The proton densities in this region are very large, approximately 100 cm^{-3}. The entry into the magnetosphere at about 2255 UT is marked by an abrupt increase in the energetic, $E \geq 5$ keV electron intensities, characteristic of the outer radiation zone, and a substantial decrease in the low energy proton densities. A further indication of entry into the magnetosphere is also provided by the electric field measurements, in Figure 3, which show an abrupt onset of continuum radiation trapped inside of the magnetosphere at 2255 UT.

A detailed investigation of the region of high plasma density immediately before the entry into the magnetosphere provides strong evidence that this region is the polar cusp. As shown in the top

panel of Figure 3 the magnetic field in this region is highly turbulent and irregular, in sharp contrast to the smooth regular field inside of the magnetosphere. However, in addition to the turbulence, a smoothly varying background component is also evident in this region. This background field is shown in greater detail by Figure 7, which gives 15 minute averages of the magnetic field vectors projected onto planes parallel and perpendicular to the meridian plane. During this pass the spacecraft orientation system was operating so the direction of the magnetic field can be determined in geomagnetic coordinates (θ_m^B is the magnetic latitude of the $\vec{B}$ field direction and φ_m^B is the magnetic longitude referenced to the magnetic meridian plane). The close correspondence of the magnetic field to the expected dipolar form is clearly evident within the magnetosphere, after 2255 UT. In the more disordered field before 2255 UT a strong dipolar component is evident in the average magnetic field direction from about 2225 to 2255 UT, with some skewing out of the meridian plane toward local dawn. Although the spin axis orientation is not optimal for determining the pitch angle distribution, inspection of the proton angular distributions in Plate 3 shows that the plasma in this region (particularly from about 2225 to 2245 UT) has a component of flow directed along the magnetic field away from the earth (maximum intensities at pitch angles near 180°). The dipolar form of the average magnetic field and the plasma flow away from the earth strongly suggest that the region from about 2225 to 2255 UT corresponds to the "entry layer" region of the polar cusp, as described by Paschmann et al. [1975]. Further evidence

identifying the region from 2225 to 2259 UT as the polar cusp is given by the plasma wave data in Figure 3 which shows the occurrence of intense ULF-ELF magnetic field noise throughout this region, with a sharp cutoff at the polar cusp/magnetosphere boundary. As previously shown on passes which enter the polar cusp from the polar cap, this noise usually provides a reliable indication of the polar cusp. A detailed magnetic field spectrum of the ULF-ELF magnetic noise is shown in Figure 8, from about 2249 to 2252 UT near the time of maximum intensity. This spectrum shows clear evidence of an upper frequency cutoff near the electron gyrofrequency, f_g^-.

Although the boundary between the polar cusp and the magnetosphere on this pass is distinct and well defined the boundary between the magnetosheath and the polar cusp is much more difficult to identify. Almost all of the available measurements show some distinctive change in characteristics between about 2220 and 2230 UT, indicative of a transition between the magnetosheath and the polar cusp. However, the location of the transition depends on the phenomena being considered. The magnetic field data in Figures 3 and 7 show a distinct transition in direction from 2220 to 2230 UT, changing from a generally southward field before 2220 UT to a dipolar field after 2230 UT. The wave magnetic field data in the middle panel of Figure 3 also show a distinct change in character, from impulsive narrow-band bursts at ~ 100-300 Hz before 2220 UT, to the broad-band ULF-ELF magnetic noise after about 2230 UT. Detailed examination of the frequency-time spectrograms of the narrow-band bursts shows that this noise consists

of "lion's roar", a type of whistler-mode emission commonly found throughout the magnetosheath [Smith et al., 1969; Smith and Tsurutani, 1976]. A typical frequency-time spectrum of the lion's roar emissions, from 2135 to 2137 UT, is shown in Figure 9, expanded to a time scale suitable for resolving the individual bursts. Since lion's roar emissions are known to be a characteristic feature of the magnetosheath, the presence of these emissions before about 2220 UT provides strong evidence that this region is the magnetosheath. Further evidence of the transition from the polar cusp to the magnetosheath is given by the electric field measurements in Figure 10. Electrostatic electron cyclotron waves at $f \simeq f_g^-$ and broad-band electrostatic noise are clearly evident in Figure 10 from about 2230 to 2255 UT, in the polar cusp region. Although the electron cyclotron waves do not delineate the polar cusp/polar cap boundary (see Figure 5), previous studies of electrostatic waves in the magnetosheath [Rodriguez and Gurnett, 1975] never show the occurrence of electron cyclotron waves in the magnetosheath. Since these waves are found in the polar cusp but not in the magnetosheath the onset of electron cyclotron waves at 2230 UT provides a further indication of a transition from the magnetosheath to the polar cusp.

Day 31, 1976

The fourth representative pass, in Figure 4, is a low-altitude pass over the southern polar cap near the noon-midnight meridian. This pass was selected to illustrate the plasma wave phenomena in the polar cusp close to the earth, at radial distances less than

2.0 R_e. The LEPEDEA data for this pass, in Plate 4, show the electron and proton intensities as the spacecraft crosses over the polar cap from about 1704 to 1717 UT and through the polar cusp from about 1717 to 1720 UT. The polar cusp is again indicated by an intense flux of the low-energy, 200 eV to 2.0 keV, protons. As can be seen from Plate 4, the proton angular distribution has a distinct maximum at pitch angles near 180°, which in the southern hemisphere corresponds to a flow of plasma downward toward the earth. The entry into the durable trapping region of the outer magnetosphere is clearly indicated by the abrupt increase in the energetic, $E > 5$ keV, electron intensities at about 1720 UT. In the polar cusp, from 1717 to 1720 UT, intense fluxes of low-energy electrons are also evident in the upper panel of Plate 4. These electrons have an angular distribution sharply peaked at pitch angles of about 45° (corresponding to a motion upward, away from the earth), suggesting that these electrons are being accelerated by an interaction with the polar cusp at some point below the spacecraft.

The plasma waves observed during this low-altitude polar cusp crossing are displayed in Figure 4 and exhibit many of the same basic characteristics evident at intermediate and high altitudes. Strong ULF-ELF magnetic noise is present in the polar cusp at frequencies below about 178 Hz. In the electric field data, strong electric fields are detected over the entire frequency range covered, from 1.78 Hz to 178 kHz. At high frequencies, above about 1.0 kHz, this noise consists of auroral hiss. As in the high altitude observations the auroral hiss is not confined to the immediate vicinity of the cusp, but spreads

out over a wide range of latitudes, particularly on the polarward side of the cusp. Auroral hiss is also detected from the nightside auroral region and merges with the dayside auroral hiss to form a nearly continuous band of noise over the entire polar cap. At low frequencies, less than about 1.0 kHz, the auroral hiss merges into an intense band of noise comparable to the "broad-band electrostatic noise" observed at high altitudes. The broad-band electrostatic noise is much more localized than the auroral hiss and can be clearly identified with two distinct regions, the polar cusp on the dayside of the earth and the auroral zone on the night side of the earth. In the polar cusp the electric field strength of the broad-band electrostatic noise, integrated from 1.78 Hz to 178 kHz, is about 15 mV m^{-1}. In the night side auroral zone the broad-band electrostatic noise is even more intense, with a broad-band electric field strength exceeding 100 mV m^{-1}.

III. FURTHER ANALYSIS AND DISCUSSION

A. ULF-ELF Magnetic Noise

As shown by the examples in Figures 1-4 and numerous other passes which have been investigated the ULF-ELF magnetic noise is nearly always present in the polar cusp. At intermediate and low altitudes the region of occurrence of this noise has a very close correspondence with the enhanced 200 eV to 2 keV proton intensities which are taken to be the primary signature of the polar cusp at these altitudes. At higher altitudes the ULF-ELF magnetic noise provides a good indicator of the polar cusp/magnetosphere boundary, but does not provide a good indicator of the polar cusp/magnetosheath boundary because of the presence of similar broad-band ULF-ELF noise throughout the magnetosheath [Smith et al., 1967]. Usually the ULF-ELF magnetic noise is more intense in the polar cusp, however the intensity often varies gradually from the polar cusp into the magnetosheath, as in Figure 3, so that a well-defined boundary cannot be identified.

To obtain a better impression of the region in which the ULF-ELF magnetic noise is observed a survey has been conducted of all of the data available from Hawkeye 1 within $\pm$ 2 hours of the noon-midnight meridian plane. The results of this survey are shown in Figure 11, which shows all of the measurements with magnetic field strengths exceeding the instrument noise level (see Figure 8) by more than 10 db

from 1.78 to 56.2 Hz. This threshold level is set sufficiently low to include both the relatively weak magnetosheath ULF-ELF magnetic noise as well as the more intense noise in the polar cusp. Geomagnetic coordinates are used in Figure 11, with the Z_m axis parallel to the earth's dipole axis and the sun in the X_m, Z_m plane. At large radial distances from the earth, $\geq$ 10 R_e, the ULF-ELF magnetic noise is mainly associated with the magnetosheath. On the night side of the earth the large variations in the magnetopause boundary position are mainly due to seasonal effects, since geomagnetic coordinates do not provide a good representation of the magnetopause, particularly on the night side of the earth. Closer to the earth the outlines of the polar cusp region, penetrating in close to the earth, are clearly evident. The low-altitude cutoff in the northern hemisphere, at about 5 R_e, is due to limitations in the orbital coverage, since passes through the polar cusp field lines do not occur at radial distances less than about 5 R_e in the northern hemisphere. Several polar cusp encounters are evident in the southern hemisphere at radial distances less than about 2 R_e. To take into account the effects of the orbital coverage a detailed statistical analysis has been performed. The results of this analysis are illustrated in Figure 12, which shows the frequency of occurrence as a function of magnetic latitude and magnetic local time in fixed radial distance intervals. The general outlines of the polar cusp region are clearly evident, increasing in angular size with increasing distance from the earth. In the 5.01 $R_e \leq R < 6.31$ R_e radial distance interval the number of data points near the cusp is

too small for good statistical accuracy, ~ 10 samples per box. Insufficient data is available at radial distances less than 5.01 R_e to provide a meaningful statistical analysis.

In considering the possible origin of the ULF-ELF magnetic noise an important questions to be considered is whether the noise is caused by wh stler-mode waves, which is the only propagating electromagnetic mode in this frequency range, or by quasi-stationary magnetic perturbations which are being convected by the spacecraft. An argument can be made for the presence of whistler-mode waves on the basis of the upper frequency range of the noise, which is frequently found to extend up to, but never to exceed, the electron gyrofrequency, f_g^-, (see Figure 8, for example). As is well known, the whistler-mode has an upper frequency cutoff at the electron gyrofrequency. Although the correspondence of the upper cutoff frequency to the local electron gyrofrequency is strongly suggestive of the whistler mode it is desirable to have a more definitive determination of the mode of propagation. Attempts have been made to measure the electric to magnetic field ratio to determine if this ratio is consistent with the whistler mode index of refraction, however the low frequency component of the broad-band electrostatic noise is generally too strong to permit detection of the electric field of the ULF-ELF noise, assuming that it is whistler-mode noise. It is possible that the ULF-ELF magnetic noise and the broad-band electrostatic noise are somehow closely related, since the spectrums of both types of noise are quite similar, decreasing rapidly in intensity with increasing

frequency with a power law index of about -2 to -3. However, comparisons of the electric to magnetic field ratios vary over a wide range, $cB/E \simeq 1$ to 30, and are generally too small to be in agreement with the whistler-mode index of refraction. Inspection of the electron angular distributions in the region where the ULF-ELF magnetic noise is observed, as for example from 1422 to 1434 UT in Plate 1 or from 1712 to 1800 UT in Plate 2, usually does not indicate a sufficient anisotropy to generate whistler-mode waves according to the mechanism of Kennel and Petschek [1966]. The measured anisotropy of the electron angular distributions within the energy range ~ 100 eV to 1 keV is less than a factor of 2. However, these observations do not preclude the possibility that narrow field-aligned electron beams with angular dimensions substantially lesser than those of the plasma analyzer, ~ 25°, are present in the polar cusp at these times. Several other mechanisms, based on shear-driven instabilities [D'Angelo, 1973] and drift-wave instabilities, exist which could generate whistler-mode waves and the possible role of these mechanisms in generating the ULF-ELF magnetic noise needs further investigation.

B. Broad-Band Electrostatic Noise

Electrostatic noise with characteristics very similar to the broad-band electrostatic noise in the polar cusp has been found in the distant magnetotail [Gurnett et al., 1976], along the auroral field lines extending into the distant magnetotail [Gurnett and Frank, 1977] and in the magnetosheath [Rodriguez and Gurnett, 1975]. The broad-band electrostatic noise in the polar cusp appears to be

essentially the dayside extension of a region of broad-band electrostatic noise which extends along the auroral field lines at all local times, following the auroral oval around the earth. This viewpoint is supported by the frequency of occurrence diagram in Figure 13 [from Gurnett and Frank, 1977], which shows the distribution of broad-band electrostatic noise as a function of magnetic latitude and magnetic local time at radial distances from 5.01 to 6.31 R_e. These data show that the broad-band electrostatic noise extends all the way around the earth in a narrow region bounded by L-values from about 8 to 12 on the night side of the earth, and by L-values from about 18 to 30 on the day side of the earth. This noise is therefore not unique to the polar cusp and is probably associated with some other feature of the auroral field lines, such as field-aligned currents, which also occurs in the polar cusp. Comparisons of electric field spectrums of the broad-band electrostatic noise in the polar cusp with similar spectrums on the night side of the earth show that the night side noise is much more intense. Typical maximum broad-band electric field strengths are about 3.0 mV m^{-1} in the polar cusp, compared to about 30 mV m^{-1} on the night side of the earth. The low altitude pass in Figure 4 also shows this marked difference in the intensity of the broad-band electrostatic noise between the night side auroral zone and the polar cusp.

High-time resolution spectrograms of the broad-band electrostatic noise, such as in Figure 14, from the polar cusp crossing on Day 186, 1974, show that the noise consists of many short impulsive bursts with very little frequency structure. As shown in Figures 1

to 4, this noise often extends with weak but detectable intensities up to frequencies as high as 30 to 100 kHz. The upper frequency limit of the broad-band electrostatic noise appears to be somewhat higher in the polar cusp than on the night side of the earth, which is typically about 10 to 20 kHz. This difference in the upper frequency limit is believed to be due to the higher plasma densities, hence electron plasma frequency, f_p^-, in the polar cusp compared to the night side auroral field lines. Typically the broad-band electrostatic noise does not extend significantly above the local electron plasma frequency as determined from the charged particle measurements.

At the present time the origin of the broad-band electrostatic noise is not adequately understood. Ashour-Abdalla and Thorne [1977] have suggested that this noise consists of high harmonics of an electrostatic ion-cyclotron instability, smeared by doppler shift effects to give an essentially continuous spectrum. This model has recently been further developed and investigated by Swift [1977] to explain large potential drops along the auroral field lines. Other possibilities, previously suggested by Scarf et al. [1972] and Fredricks et al. [1973] to explain similar impulsive electrostatic waves detected in the polar cusp by OGO 5, include the ion-acoustic instability or the Buneman instability [Buneman, 1958].

C. Electrostatic Electron Cyclotron Waves

Narrow-band electrostatic emissions near the local electron gyrofrequency, f_g^-, comparable to those illustrated in Figure 5, are commonly observed in the polar cusp. These emissions, which are

referred to as electron cyclotron waves, always occur at a frequency slightly above the electron gyrofrequency, typically $f \simeq 1.1\ f_g^-$ to $1.2\ f_g^-$. Occasionally an emission can also be detected near the second and higher harmonics of the electron gyrofrequency, nf_g^-, as in Figure 14. The electric field strength of these waves is normally very weak, typically only ten to one hundred $\mu V\ m^{-1}$. As evident in Figure 5 the electron cyclotron waves are not uniquely associated with the polar cusp, but often extend into the magnetosphere and polar cap regions on either side of the cusp. These waves are not however normally detected in the magnetosheath and in some cases the termination of these waves provides an indication of the polar cusp/magnetosheath transition, as in Figure 10. Often the electron cyclotron emissions are most intense and clearly defined in the region of steady magnetic fields just inside the magnetosphere and are weaker and more diffuse in the polar cusp (see Figures 10 and 14).

Electrostatic waves of this type, near harmonics of the electron gyrofrequency, have been previously observed in the inner regions of the earth's magnetosphere [Kennel et al., 1970; Fredricks and Scarf, 1973; Shaw and Gurnett, 1975] and in the distant magnetotail [Scarf et al., 1974; Gurnett et al., 1976]. Usually, these waves occur near half-integral harmonics of the electron gyrofrequency, $(n + 1/2)f_g^-$. Although the waves observed in polar cusp are closer to the harmonics than half-integral harmonics, they are still believed to belong to the same general class of electrostatic electron cyclotron instabilities studied by Young et al. [1973], Ashour-Abdalla and Kennel [1976], and others.

D. Auroral Hiss

Whistler-mode auroral hiss emissions, comparable to those in Figures 1 and 4, are a common feature of the polar cusp crossings observed by Hawkeye 1. The intensity and frequency of occurrence of these emissions generally increase with decreasing altitude. Near the earth, at $R \leq 2\ R_e$, auroral hiss is detected on nearly every pass through the polar cusp. At high altitudes, $R \geq 6\ R_e$, the auroral hiss distribution has a distinct latitudinal asymmetry, with the auroral hiss only occurring on the poleward side of the polar cusp, as in Figure 5, for example. A similar asymmetry is also observed for auroral hiss emissions on the night side of the earth [compare with Figure 5 in Gurnett and Frank, 1977]. This latitudinal asymmetry at high altitudes is considered somewhat unusual, since at low altitudes the auroral hiss usually has a latitudinally symmetric structure, often with a characteristic v-shaped low frequency cutoff [Gurnett and Frank, 1972]. Since the auroral hiss detected at high altitude appears to be propagating upwards away from the earth, it seems most likely that this asymmetry is an absorption effect, with strong absorption on the magnetosphere side of the cusp and little or no absorption in the polar cap. Such an asymmetry in the whistler mode absorption is not unexpected, since resonant damping processes should be much stronger in the hot magnetospheric plasma compared to the relatively cold plasma in the polar cusp. Evidence of cyclotron damping in the polar cusp is in fact indicated by the sharp upper cutoff of the auroral hiss in Figure 5, at about $f \simeq 0.85\ f_g^-$. The

electron energy responsible for this absorption, computed from the whistler-mode resonance condition [Kennel and Petschek, 1966],

$$E_R = \frac{B^2}{8\pi N} \left(\frac{f_g^-}{f}\right)\left(1 - \frac{f}{f_g^-}\right)^3 ,$$

using $f/f_g^- = 0.85$, $N = 1$ electron cm^{-3} and $B = 100$ gammas, is estimated to be about 100 eV. Since substantial absorption probably occurs well before the resonance energy reaches the average energy of the electrons, this energy implies an average electron energy of a few tens of eV. Energies of ~ 10 to 50 eV are believed to be typical of the relatively cold, low density, polar cap plasma.

At low altitudes substantial evidence has been presented showing that auroral hiss is produced by large fluxes of low energy, ~ 100 eV, electrons in the polar cusp [Gurnett and Frank, 1972; Laaspere and Hoffman, 1976]. In general the Hawkeye 1 observations at high altitudes continue to support this relationship, since substantial fluxes of low-energy, ~ 100 eV, electrons are a common feature of the polar cusp. Detailed comparisons however do not show as clear a relationship between the ~ 100 eV electron intensities and the occurrence of auroral hiss as in the low altitude observations. Since the source of the auroral hiss is evidently far below the spacecraft, significant acceleration of these electrons may be occurring between the spacecraft and the region where the auroral hiss is generated, which would tend to obscure the relationship. Just how the auroral hiss generation is related to these acceleration processes and the exact altitude range in which the radiation is produced remain quite uncertain.

IV. CONCLUSION

The principal types of plasma waves observed by Hawkeye 1 in and near the polar cusp are (1) ULF-ELF magnetic noise, (2) broad-band electrostatic noise, (3) electrostatic electron cyclotron waves, and (4) auroral hiss. The region of occurrence of these waves and their relation to the major regions of the magnetosphere are summarized in Figure 15. Of these plasma wave phenomena only the ULF-ELF magnetic noise can be considered to be uniquely associated with the polar cusp. All of the other types of waves either occur too sporadically or are not sufficiently localized within the cusp to be useful as an indicator of the polar cusp location. The Hawkeye 1 observations of the ULF-ELF magnetic noise are in close agreement with the earlier HEOS 2 measurements. The main differences are that the Hawkeye 1 measurements of the ULF-ELF noise extend to higher frequencies, providing evidence of an upper cutoff near the electron gyrofrequency, and that the noise tends to occur throughout the polar cusp rather than just at the boundaries of the cusp as stressed by D'Angelo [1973] and D'Angelo *et al.* [1974]. This last difference is not to be strongly emphasized, since we do on some occasions find that the maximum intensities occur near the cusp boundaries (particularly at the cusp/magnetosphere boundary, as in Figure 3). However, many other cases occur in which the ULF-ELF noise is essentially

uniform throughout the cusp (as in Figures 1 and 2). Also, at high altitudes, near the magnetosheath, it is very difficult to clearly identify the magnetosheath/cusp interface, so there is some uncertainty in the relationship of the ULF-ELF noise to the polar cusp boundaries in this region, depending on how the boundaries are defined.

The primary interpretational questions which remain involving the ULF-ELF magnetic noise are concerned with the mode of propagation and the mechanism for generating these waves. D'Angelo et al. [1974] regard this noise as turbulence generated by the Kelvin-Helmholtz instability. In this interpretation the turbulence is not identified with any particular plasma wave mode but represents a steady state noise spectrum arrived at by the non-linear cascading of the turbulent energy to higher and higher wave numbers. On the other hand, the fact that the spectrum of the ULF-ELF noise often extends up to near the electron gyrofrequency, but never seems to exceed this frequency suggests that the turbulence consists of whistler-mode waves. Unfortunately, it has not been possible to confirm this mode identification by measuring the electric to magnetic field ratio. If the ULF-ELF noise does consist of whistler-mode waves it does not appear that the waves are produced by the well-known cyclotron resonance instability discussed by Kennel and Petschek [1966], since the noise is often observed in regions with a nearly isotropic electron distribution. Other methods of generating whistler-mode turbulence in the polar cusp need to be investigated.

Of the three remaining types of plasma wave analyzed, broad-band electrostatic noise, electron cyclotron waves and auroral hiss, none are uniquely associated with the polar cusp, even though they are frequently observed in the cusp. All of these waves are detected primarily by their electric field, since they are essentially electrostatic, with electric field energy densities exceeding the magnetic field energy density. As can be seen from Figures 1-4, it is usually not possible to uniquely identify the polar cusp on the basis of the electric field measurements alone, since all of these waves extend to varying degrees into the region outside the cusp. Of these waves the weak high frequency, $\geq$ 10 kHz, component of the broad-band electrostatic noise appears to be most closely confined to the polar cusp. At lower frequencies, $\leq$ 10 kHz, the broad-band electrostatic noise often extends well beyond the polar cusp boundaries, as in Figures 1 and 3. Similarly, the electrostatic electron cyclotron waves often extend into the magnetosphere and polar cap regions on either side of the cusp. The broad region of occurrence of these waves indicates that the particular feature of the particle distribution function required for the generation of these waves is not confined to the polar cusp, but also occurs in the regions adjacent to the cusp. The auroral hiss emissions generated within the polar cusp are detected large distances beyond the cusp boundaries, which is not surprising since these emissions are whistler-mode waves which propagate with relatively little attenuation in the magnetospheric plasma.

The only previous electric field measurements which can be compared with these electric field measurements are from the OGO 5 spacecraft [Scarf et al., 1972; Fredricks et al., 1973]. The OGO 5 observations are all from a single large magnetic storm on November 1, 1968, which displaced the polar cusp to a sufficiently low latitude to be detected by OGO 5. The OGO 5 cusp observations are characterized by very large electric field intensities, 10 to 40 mV m^{-1}, with strong excitation of a number of electrostatic ($f \simeq f_{LHR}$, f_g^-, f_p^-, and f_p^+) wave modes [Scarf et al., 1972]. Although some of the wave modes detected by Hawkeye 1 can be regarded as broadly similar to the OGO 5 observations, in general the wave intensities detected at high altitudes by Hawkeye 1 are substantially less intense than those detected by OGO 5. The similarities include observations of auroral hiss with a low frequency cutoff near the local lower-hybrid-resonance frequency, broad-band bursts of electrostatic noise (although of substantially lower intensity for Hawkeye), and electrostatic waves near the electron gyrofrequency. The large electric field intensities detected by OGO 5 in the polar cusp are not necessarily considered to be in disagreement with the Hawkeye 1 measurements because of the unusual nature of the OGO 5 event (K_p = 8+) and the fact that the OGO 5 polar cusp crossings occurred at radial distances (3 to 5 R_e) closer to the earth than for Hawkeye 1.

In comparison with the plasma wave phenomen occurring in other regions of the earth's magnetosphere, the plasma waves observed in the polar cusp bear a strikingly close resemblance to similar

plasma wave phenomena in the magnetosheath. Magnetic noise, comparable to the ULF-ELF magnetic noise found in the polar cusp, also occurs throughout the magnetosheath [Smith et al., 1967]. This magnetosheath magnetic noise has a spectrum varying approximately as f^{-3} and extends from a few Hz to about 300 Hz. The intensity of the magnetosheath noise is highly variable, and on the average is slightly weaker, by about a factor of 3 to 10, than the noise in the polar cusp. Electrostatic noise, comparable to the broad-band electrostatic noise found in the polar cusp, is also observed throughout the magnetosheath [Rodriguez and Gurnett, 1973; Rodriguez, 1977]. The magnetosheath electrostatic noise is a broad-band electrostatic emission which extends from frequencies of a few Hz up to near the electron plasma frequency at about 20 to 30 kHz. The intensity of the magnetosheath electrostatic noise is also highly variable, and is usually most intense in the region immediately behind the shock, decreasing in amplitude with increasing distance from the shock. A similar type of broad-band electrostatic noise is also observed in the distant magnetotail at the outer boundaries of the plasma sheet [Gurnett et al., 1976] extending along the auroral field lines to low altitudes in the ionosphere [Gurnett and Frank, 1977]. Although close similarities exist between the plasma waves in the magnetosheath and polar cusp, important differences are also evident. Narrow-band "lion's roar" emissions, which are commonly observed throughout the magnetosheath, are almost never observed in the polar cusp and

electrostatic electron cyclotron waves, which are commonly observed in the polar cusp, are not normally observed in the magnetosheath. The reasons for these similarities and differences are not fully understood and need further investigation.

ACKNOWLEDGMENTS

The authors wish to express their thanks to J. A. Van Allen for the use of the magnetic field data from Hawkeye 1, to R. R. Anderson for his assistance in the data processing and to N. D'Angelo, J. Craven, and K. Ackerson for their helpful discussions concerning the data interpretation. The research at the University of Iowa was supported by the National Aeronautics and Space Administration through Grants NGL-16-001-002 and NGL-16-001-043, through Contracts NAS1-11257 and NAS1-13129 with Langley Research Center, and by the U. S. Office of Naval Research through Contract N00014-76-C-0016.

REFERENCES

Ashour-Abdalla, M., and C. F. Kennel, Convective cold upper hybrid instabilities, Magnetospheric Particles and Fields, edited by B. M. McCormac, D. Reidel, Dordrecht, The Netherlands, 181, 1976.

Ashour-Abdalla, M., and R. M. Thorne, The importance of electrostatic ion-cyclotron instability for quiet-time proton auroral precipitation, Geophys. Res. Lett., 1, 45, 1977.

Buneman, O., Instability, turbulence, and conductivity in current-carrying plasma, Phys. Rev. Lett., 1, 8, 1958.

D'Angelo, N., Ultralow frequency fluctuations at the polar cusp boundaries, J. Geophys. Res., 78, 1206, 1973.

D'Angelo, N., A. Bahnsen, and H. Rosenbauer, Wave and particle measurements at the polar cusp, J. Geophys. Res., 79, 3129, 1974.

Frank, L. A., Plasma in the earth's polar magnetosphere, J. Geophys. Res., 76, 5202, 1971.

Frank, L. A., and K. L. Ackerson, Observations of charged particle precipitation into the auroral oval, J. Geophys. Res., 76, 3612, 1971.

Fredricks, R. W., and F. L. Scarf, Recent studies of magnetospheric electric field emission above the electron gyrofrequency, J. Geophys. Res., 78, 310, 1973.

Fredricks, R. W., F. L. Scarf, and C. T. Russell, Field-aligned currents, plasma waves, and anomalous resistivity in the disturbed polar cusp, J. Geophys. Res., 78, 2133, 1973.

Gurnett, D. A., and L. A. Frank, VLF hiss and related plasma observations in the polar magnetosphere, J. Geophys. Res., 77, 172, 1972.

Gurnett, D. A., and R. R. Shaw, Electromagnetic radiation trapped in the magnetosphere above the plasma frequency, J. Geophys. Res., 78, 8136, 1973.

Gurnett, D. A., L. A. Frank, and R. P. Lepping, Plasma waves in the distant magnetotail, J. Geophys. Res., 81, 6059, 1976.

Gurnett, D. A., and L. A. Frank, A region of intense plasma wave turbulence on auroral field lines, J. Geophys. Res., 82, 1031, 1977.

Heikkila, W. J., and J. D. Winningham, Penetration of magnetosheath plasma to low altitudes through the dayside magnetospheric cusps, J. Geophys. Res., 76, 883, 1971.

Kennel, C. F., and H. E. Petschek, Limit on stably trapped particle fluxes, J. Geophys. Res., 71, 1, 1966.

Kennel, C. F., F. L. Scarf, R. W. Fredricks, J. H. McGhee, and F. V. Coroniti, VLF electric field observations in the magnetosphere, J. Geophys. Res., 75, 6136, 1970.

Kurth, W. S., M. M. Baumback, and D. A. Gurnett, Direction-finding measurements of auroral kilometric radiation, J. Geophys. Res., 80, 2764, 1975.

Laaspere, T., W. C. Johnson, and L. C. Semprebon, Observations of auroral hiss, LHR noise, and other phenomena in the frequency range 20 Hz to 540 kHz on OGO 6, J. Geophys. Res., 76, 4477, 1971.

Laaspere, T., and R. A. Hoffman, New results on the correlation between low-energy electrons and auroral hiss, J. Geophys. Res., 81, 524, 1976.

Paschmann, G., G. Haerendel, N. Schkopke, and H. Rosenbauer, Plasma and magnetic field characteristics of the distant polar cusp near local noon: the entry layer, J. Geophys. Res., 81, 2883, 1976.

Rodriguez, P., Magnetosheath electrostatic turbulence, J. Geophys. Res. (submitted for publication), 1977.

Rodriguez, P., and D. A. Gurnett, Electrostatic and electromagnetic turbulence associated with the earth's bow shock, J. Geophys. Res., 80, 19, 1973.

Rosenbauer, H., H. Grünwaldt, M. D. Montgomery, G. Paschmann, and N. Sckopke, HEOS 2 plasma observations in the distant polar magnetosphere: the plasma mantle, J. Geophys. Res., 80, 2723, 1975.

Russell, C. T., C. R. Chappell, M. D. Montgomery, M. Neugebauer, and F. L. Scarf, OGO 5 observations of the polar cusp on November 1, 1968, J. Geophys. Res., 76, 6743, 1971.

Scarf, F. L., R. W. Fredricks, I. M. Green, and C. T. Russell, Plasma waves in the dayside polar cusp, 1. Magnetospheric observations, J. Geophys. Res., 77, 2274, 1972.

Scarf, F. L., L. A. Frank, K. L. Ackerson, and R. P. Lepping, Plasma wave turbulence at distant crossings of the plasma sheet boundaries and the neutral sheet, Geophys. Res. Lett., 1, 189, 1974.

Scarf, F. L., R. W. Fredricks, M. Neugebauer, and C. T. Russell, Plasma waves in the dayside polar cusp, 2. Magnetopause and polar magnetosheath, J. Geophys. Res., 79, 511, 1974.

Shaw, R. R., and D. A. Gurnett, Electrostatic noise bands associated with the electron gyrofrequency and plasma frequency in the outer magnetosphere, J. Geophys. Res., 80, 4259, 1975.

Smith, E. J., R. E. Holzer, M. G. McLeod, and C. T. Russell, Magnetic noise in the magnetosheath in the frequency range 3-300 Hz, J. Geophys. Res., 72, 4803, 1967.

Smith, E. J., R. E. Holzer, and C. T. Russell, Magnetic emissions in the magnetosheath at frequencies near 100 Hz, J. Geophys. Res., 74, 3027, 1969.

Smith, E. J., and B. J. Tsurutani, Magnetosheath lion roars, J. Geophys. Res., 81, 2261, 1976.

Swift, D. W., Turbulent generation of electrostatic fields in the magnetosphere, J. Geophys. Res. (submitted for publication), 1977.

Young, P. S., J. D. Callen, and J. E. McCune, High-frequency electrostatic waves in the magnetosphere, J. Geophys. Res., 78, 1082, 1973.

FIGURE CAPTIONS

Figure 1 The electric and magnetic field measurements for a representative Hawkeye 1 pass through the polar cusp. The corresponding charged particle intensities for this pass are shown in Plate 1. The spacecraft enters the polar cusp from the polar cap at about 1422 UT and crosses into the magnetosphere at about 1434 UT. The approximate configuration of the magnetic field and the spacecraft trajectory are shown by the small sketch in the bottom panel. Within the polar cusp the primary plasma wave phenomena evident in these data are the ULF-ELF magnetic noise from about 1.78 Hz to 178 Hz and the high frequency components of the broad-band electrostatic noise. Small perturbations in the magnetic field, probably indicative of field-aligned currents, are also evident in the polar cusp region.

Figure 2 Another representative polar cusp crossing, similar to Figure 1, which enters the cusp from the polar cap. The corresponding charged-particle intensities are shown in Plate 2. Again the ULF-ELF magnetic noise and the high

frequency components of the broad-band electrostatic noise are present in the polar cap region. No significant magnetic field perturbations are evident in the polar cusp during this pass. The electromagnetic continuum radiation has an abrupt cutoff at the cusp/magnetosphere boundary, indicating an abrupt change in the plasma density and electron plasma frequency, f_p^-.

Figure 3 A polar cusp crossing at a slightly lower latitude than in Figures 1 and 2. The spacecraft in this case enters the cusp from the magnetosheath, without passing through the polar cap. The corresponding charged-particle intensities are shown in Plate 3. The cusp/magnetosphere boundary is quite clear and distinct, and is characterized by an abrupt decrease in the plasma density, a change from a disordered to an ordered magnetic field, an abrupt termination of the ULF-ELF magnetic noise and the onset of trapped continuum radiation at $f > f_p^-$. The magnetosheath/cusp transition is not as well-defined and is characterized by an increase in the magnetic field fluctuations in the cusp, a transition from lion's roar emissions in the magnetosheath to ULF-ELF magnetic noise in the cusp, and an increase in the intensity of the broad-band electrostatic noise.

Figure 4 A low-altitude polar cusp crossing near the noon-midnight meridian over the southern hemisphere. The corresponding charged-particle intensities are shown in Figure 4. The polar cusp is again characterized by large ULF-ELF magnetic noise and broad-band electrostatic noise intensities. Also, intense whistler-mode auroral hiss emissions are observed in the polar cusp, over the polar cap, and in the night side auroral zone.

Figure 5 High resolution frequency-time spectrograms showing further details of the electric field emissions detected during the polar cusp crossing in Figure 1. The low frequency component, $\leq$ 2.0 kHz, of the broad-band electrostatic noise is clearly evident in the polar cusp. Whistler-mode auroral hiss emissions, with a sharp upper frequency cutoff slightly below the electron gyrofrequency, f_g^-, can be seen propagating into the region on the polarward side of the cusp. Electrostatic electron cyclotron waves at $f \simeq f_g^-$ are also evident in the polar cusp. These waves also occur in the polar cap and magnetosphere.

Figure 6 Representative spectrums of the broad-band electrostatic noise and auroral hiss from Figure 1. The r.m.s. electric field strength of the broad-band electrostatic noise is about 4.8 mV m^{-1}.

Figure 7 The magnetic field directions and magnitudes for the pass in Figure 3. The magnetic fields are shown projected in a magnetic meridian (ρ_m, Z_m) plane through the spacecraft, and in a plane perpendicular to the ρ_m axis. The Z_m axis is parallel to the magnetic dipole axis of the earth. In the polar cusp, from about 2225 to 2255 UT, the magnetic field has a strong dipolar component, with some skewing of the magnetic field out of the meridian plane toward local dawn.

Figure 8 A spectrum of the peak and average magnetic field strengths of the ULF-ELF magnetic noise in Figure 3. Note the upper cutoff in the noise spectrum near the local electron gyrofrequency, f_g^-. This cutoff suggests that the ULF-ELF noise consists of whistler-mode waves.

Figure 9 A frequency-time spectrogram showing that the impulsive magnetic noise bursts before about 2225 UT in Figure 3 consist of whistler-mode lion's roar emissions. This type of emission is commonly found throughout the magnetosheath.

Figure 10 High resolution frequency-time spectrograms of the electric field emissions detected during the polar cusp

crossing in Figure 3. The electrostatic electron cyclotron waves are seen to terminate near the cusp/magnetosheath boundary.

Figure 11 The region of occurrence of the ULF-ELF magnetic noise in geomagnetic coordinates. Only events exceeding the receiver noise level (see Figure 8) by at least 10 db from 1.78 to 56.2 Hz are shown. The ULF-ELF magnetic noise in both the magnetosheath and the polar cusp usually exceed this threshold.

Figure 12 The frequency of occurrence of the ULF-ELF magnetic noise as a function of magnetic local time and magnetic latitude within specific radial distance ranges. The general outline of the polar cusp region, decreasing in angular size with decreasing radial distance, is clearly evident.

Figure 13 The frequency of occurrence of the broad-band electrostatic noise as a function of magnetic latitude and magnetic local time in the region from 5.01 to 6.31 R_e [from Gurnett and Frank, 1977]. In contrast to the ULF-ELF magnetic noise, the broad-band electrostatic noise occurs at all local times and is not uniquely related to the polar cusp region, even though it occurs in the cusp.

Figure 14 Expanded time scale spectrograms of the electron cyclotron waves and broad-band electrostatic waves near the cusp/magnetosphere boundary in Figure 10. Within the cusp the electron cyclotron waves become very diffuse and poorly defined. The broad-band electrostatic noise is seen to consist of many impulsive bursts extending across a broad range of frequencies.

Figure 15 A summary of the primary types of plasma wave phenomena observed in the polar cusp and the magnetosheath. Many of the plasma waves observed in these two regions are very similar. The main differences are that the lion's roar emissions do not occur in the polar cusp and the electrostatic electron cyclotron waves are not observed in the magnetosheath.

Note: Plates 1-4 are to be published in color.

Plate 1 The LEPEDEA data for the polar cusp crossing in Figure 1. These spectrograms display the color-coded response of the LEPEDEA as functions of the logarithm to the base 10 of the energy in eV (ordinate) and Universal Time (abscissa). The pitch angle of the particles being detected (0 to 180°) is shown at the top of each spectrogram. The region of intense low energy (500 eV

to 2 keV) proton fluxes from about 1422 to 1434 UT is the polar cusp. The maximum intensities occur at pitch angles near 0°, indicating a directed flow of protons downward along the magnetic field toward the earth.

Plate 2 The LEPEDEA data for the polar cusp crossing in Figure 2. The polar cusp is again indicated by a well-defined region of enhanced low-energy proton intensities, from about 1712 to 1800 UT. The proton angular distributions are more complex in this case, with a flow away from the earth (pitch angles near 180°) in a broad region on the poleward side of the cusp, and a flow toward the earth in a narrow region near the low latitude boundary.

Plate 3 The LEPEDEA data near the polar cusp/magnetosphere boundary in Figure 3. The spacecraft crosses from the polar cusp into the magnetosphere at about 2255 UT, coincident with a large decrease in the low-energy proton intensities and an increase in the GM tube counting rate. In the polar cusp region, before about 2245 UT, the pitch angle distribution indicates a proton flow upward along the magnetic field, away from

the earth. This region is believed to correspond to the entry layer discussed by Paschmann et al. [1976].

Plate 4 The LEPEDEA data for the low-altitude polar cusp crossing in Figure 4. The spacecraft passes over the polar cap from about 1704 to 1717 UT and through the polar cusp from about 1717 to 1720 UT. The polar cusp region is again indicated by an intense flux of low-energy protons. The pitch angle distribution indicates a proton flow downward toward the earth.

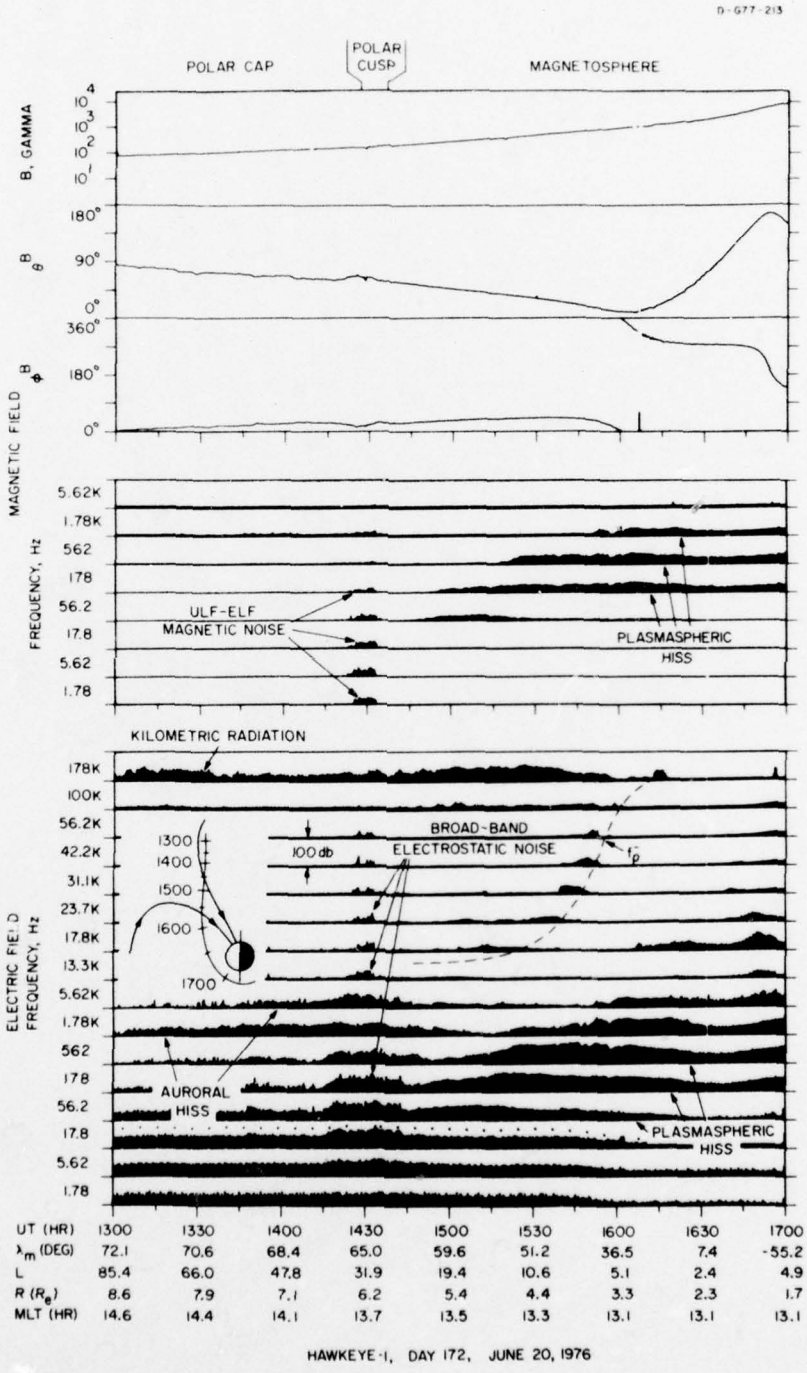
D-677-213
POLAR CAP
POLAR CUSP
MAGNETOSPHERE
MAGNETIC FIELD
B, GAMMA
10^4
10^3
10^2
10^1
B_θ
180°
90°
0°
B_ϕ
360°
180°
0°
FREQUENCY, Hz
5.62K
1.78K
562
178
56.2
17.8
5.62
1.78
ULF-ELF MAGNETIC NOISE
PLASMASPHERIC HISS
KILOMETRIC RADIATION
ELECTRIC FIELD FREQUENCY, Hz
178K
100K
56.2K
42.2K
31.1K
23.7K
17.8K
13.3K
5.62K
1.78K
562
178
56.2
17.8
5.62
1.78
1300
1400
1500
1600
1700
100 db
BROAD-BAND ELECTROSTATIC NOISE
f_p
AURORAL HISS
PLASMASPHERIC HISS
UT (HR) 1300 1330 1400 1430 1500 1530 1600 1630 1700
λ_m (DEG) 72.1 70.6 68.4 65.0 59.6 51.2 36.5 7.4 -55.2
L 85.4 66.0 47.8 31.9 19.4 10.6 5.1 2.4 4.9
R (R_e) 8.6 7.9 7.1 6.2 5.4 4.4 3.3 2.3 1.7
MLT (HR) 14.6 14.4 14.1 13.7 13.5 13.3 13.1 13.1 13.1
HAWKEYE-1, DAY 172, JUNE 20, 1976

Figure 1

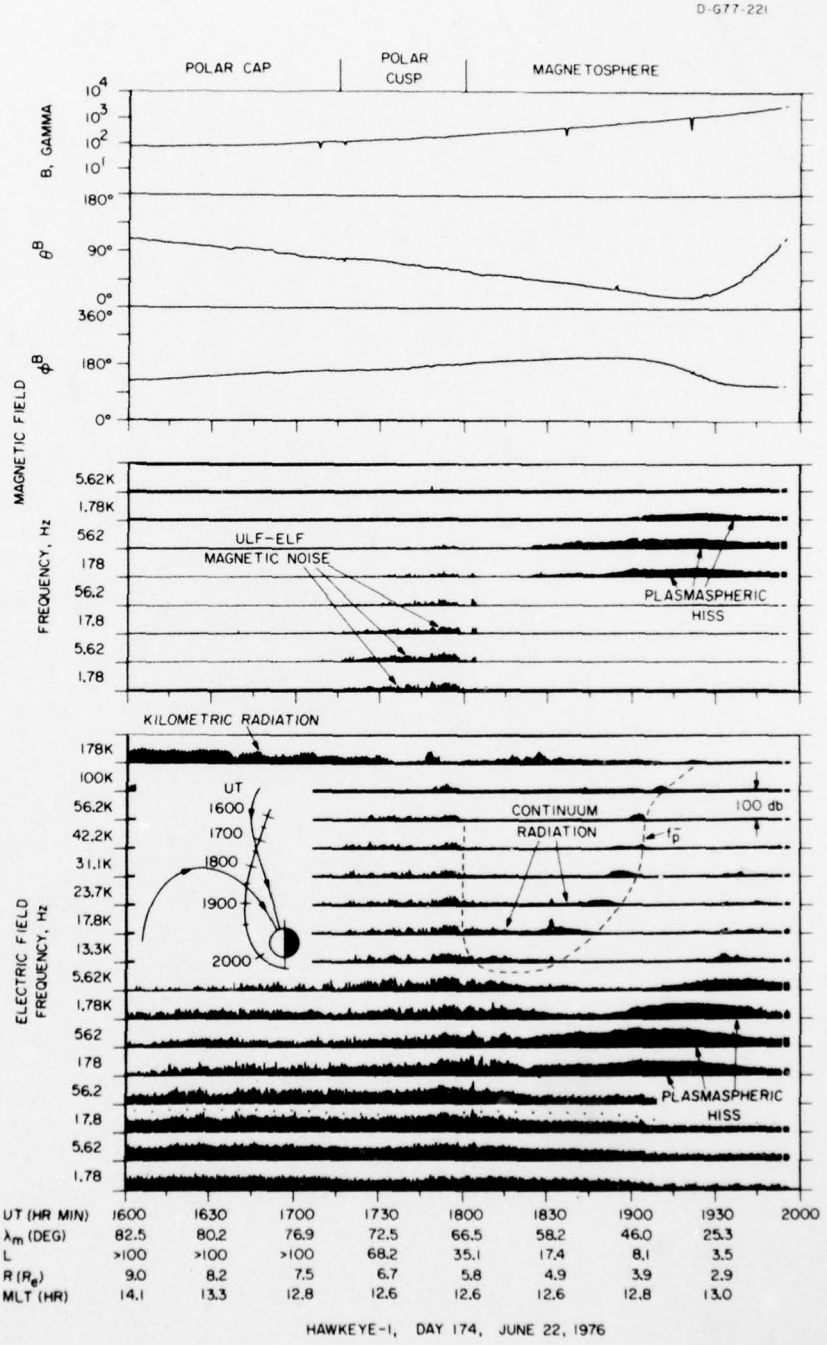
D-G77-221
POLAR CAP
POLAR CUSP
MAGNETOSPHERE
MAGNETIC FIELD
B, GAMMA
10^4
10^3
10^2
10^1
θ^B
180°
90°
0°
ϕ^B
360°
180°
0°
FREQUENCY, Hz
5.62K
1.78K
562
178
56.2
17.8
5.62
1.78
ULF-ELF MAGNETIC NOISE
PLASMASPHERIC HISS
KILOMETRIC RADIATION
ELECTRIC FIELD FREQUENCY, Hz
178K
100K
56.2K
42.2K
31.1K
23.7K
17.8K
13.3K
5.62K
1.78K
562
178
56.2
17.8
5.62
1.78
UT
1600
1700
1800
1900
2000
CONTINUUM RADIATION
100 db
f_p
PLASMASPHERIC HISS
UT (HR MIN) 1600 1630 1700 1730 1800 1830 1900 1930 2000
λ_m (DEG) 82.5 80.2 76.9 72.5 66.5 58.2 46.0 25.3
L >100 >100 >100 68.2 35.1 17.4 8.1 3.5
R (R_e) 9.0 8.2 7.5 6.7 5.8 4.9 3.9 2.9
MLT (HR) 14.1 13.3 12.8 12.6 12.6 12.6 12.8 13.0
HAWKEYE-1, DAY 174, JUNE 22, 1976

Figure 2

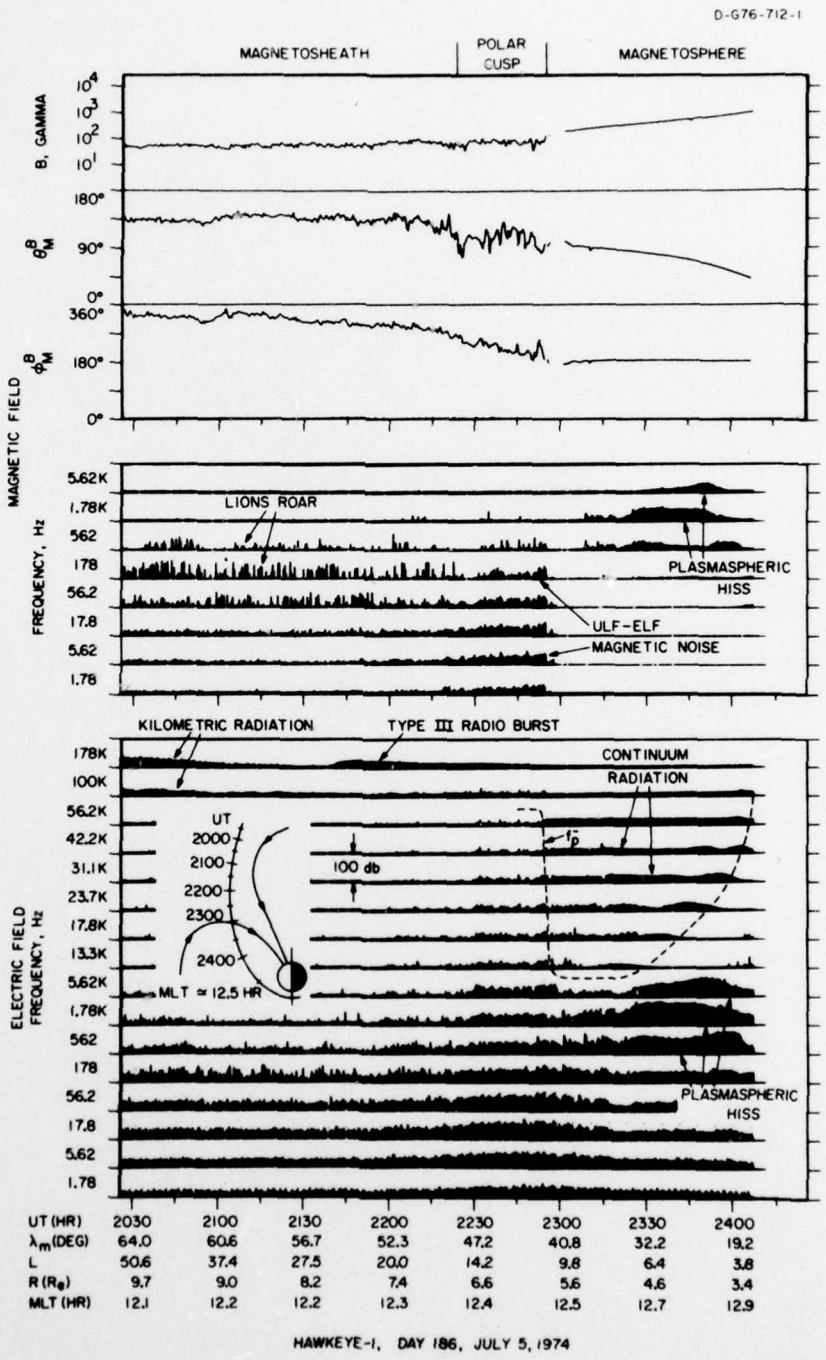
D-G76-712-1
MAGNETOSHEATH
POLAR CUSP
MAGNETOSPHERE
B, GAMMA
θ_M^B
ϕ_M^B
MAGNETIC FIELD
FREQUENCY, Hz
LIONS ROAR
PLASMASPHERIC HISS
ULF-ELF MAGNETIC NOISE
KILOMETRIC RADIATION
TYPE III RADIO BURST
CONTINUUM RADIATION
UT
2000
2100
2200
2300
2400
MLT ≃ 12.5 HR
100 db
f_p
ELECTRIC FIELD FREQUENCY, Hz
PLASMASPHERIC HISS
UT (HR) 2030 2100 2130 2200 2230 2300 2330 2400
λ_m(DEG) 64.0 60.6 56.7 52.3 47.2 40.8 32.2 19.2
L 50.6 37.4 27.5 20.0 14.2 9.8 6.4 3.8
R (R_e) 9.7 9.0 8.2 7.4 6.6 5.6 4.6 3.4
MLT (HR) 12.1 12.2 12.2 12.3 12.4 12.5 12.7 12.9
HAWKEYE-1, DAY 186, JULY 5, 1974

Figure 3

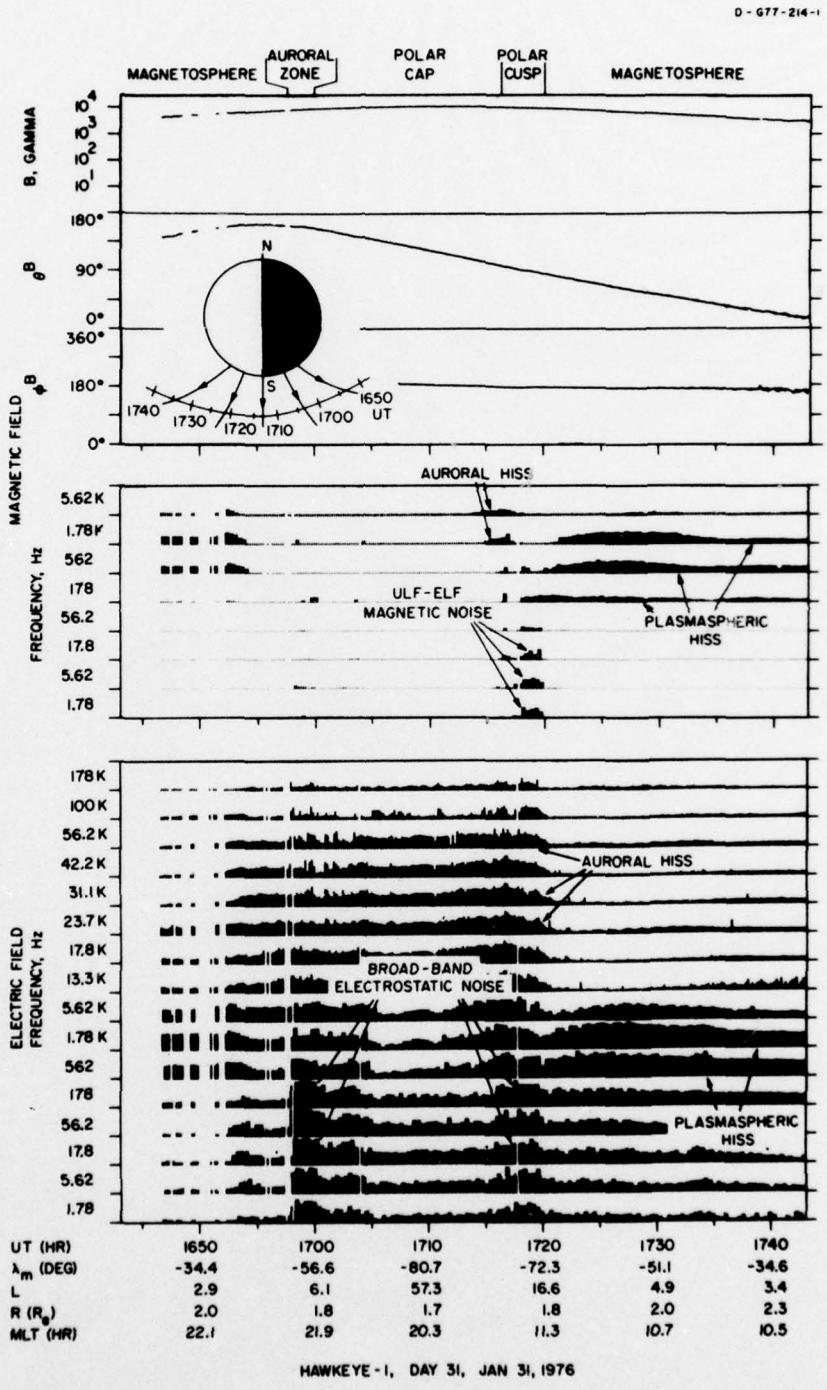
D - G77 - 214 - 1
MAGNETOSPHERE
AURORAL ZONE
POLAR CAP
POLAR CUSP
MAGNETOSPHERE
B, GAMMA
MAGNETIC FIELD
N
S
1740
1730
1720
1710
1700
1650 UT
AURORAL HISS
FREQUENCY, Hz
ULF-ELF MAGNETIC NOISE
PLASMASPHERIC HISS
ELECTRIC FIELD FREQUENCY, Hz
AURORAL HISS
BROAD-BAND ELECTROSTATIC NOISE
PLASMASPHERIC HISS
UT (HR) 1650 1700 1710 1720 1730 1740
λm (DEG) -34.4 -56.6 -80.7 -72.3 -51.1 -34.6
L 2.9 6.1 57.3 16.6 4.9 3.4
R (Re) 2.0 1.8 1.7 1.8 2.0 2.3
MLT (HR) 22.1 21.9 20.3 11.3 10.7 10.5
HAWKEYE-1, DAY 31, JAN 31, 1976

Figure 4

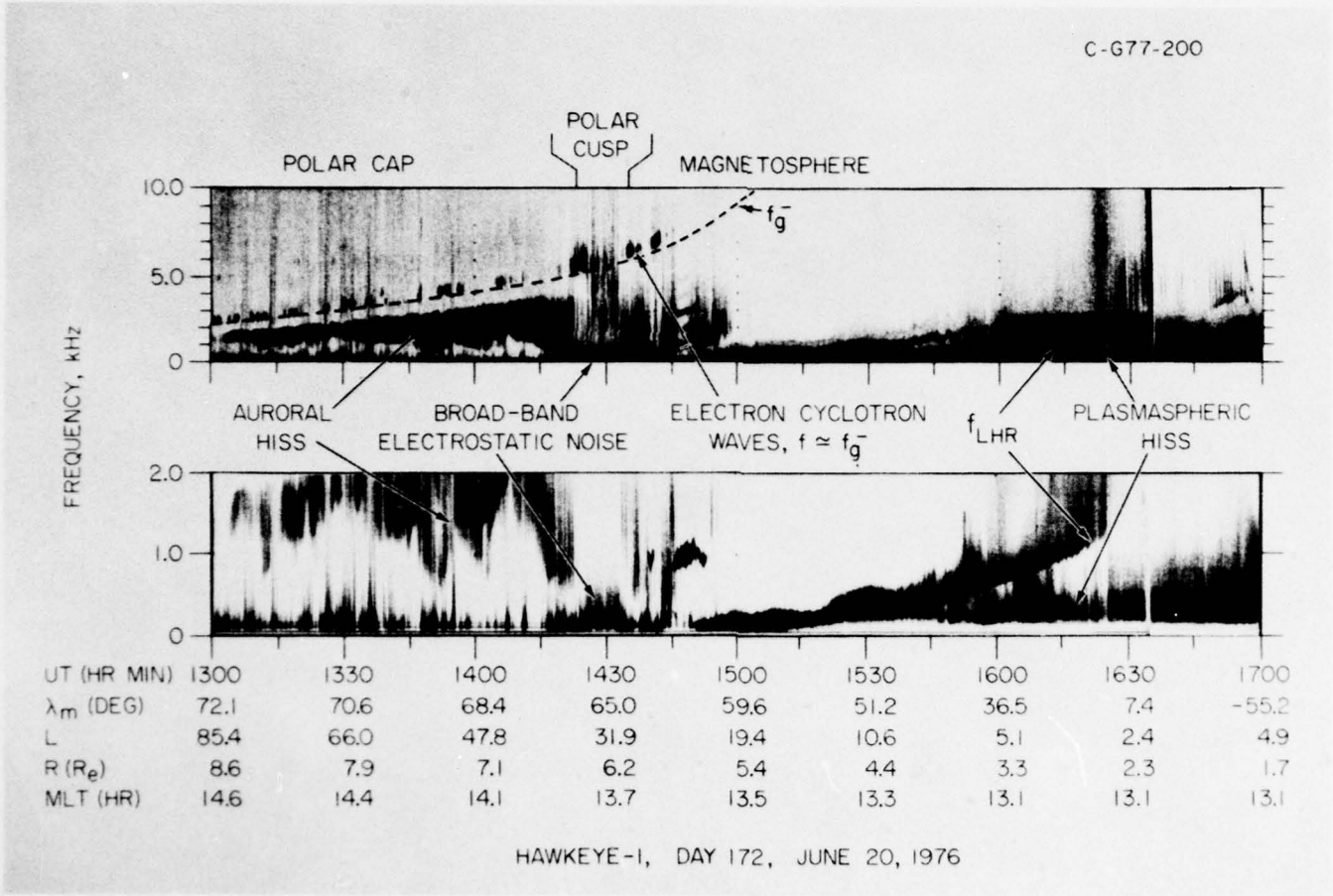
C-G77-200
POLAR CAP
POLAR CUSP
MAGNETOSPHERE
10.0
5.0
0
f_g^-
FREQUENCY, kHz
AURORAL HISS
BROAD-BAND ELECTROSTATIC NOISE
ELECTRON CYCLOTRON WAVES, $f \simeq f_g^-$
f_{LHR}
PLASMASPHERIC HISS
2.0
1.0
0
UT (HR MIN) 1300 1330 1400 1430 1500 1530 1600 1630 1700
λ_m (DEG) 72.1 70.6 68.4 65.0 59.6 51.2 36.5 7.4 -55.2
L 85.4 66.0 47.8 31.9 19.4 10.6 5.1 2.4 4.9
R (R_e) 8.6 7.9 7.1 6.2 5.4 4.4 3.3 2.3 1.7
MLT (HR) 14.6 14.4 14.1 13.7 13.5 13.3 13.1 13.1 13.1
HAWKEYE-I, DAY 172, JUNE 20, 1976

Figure 5

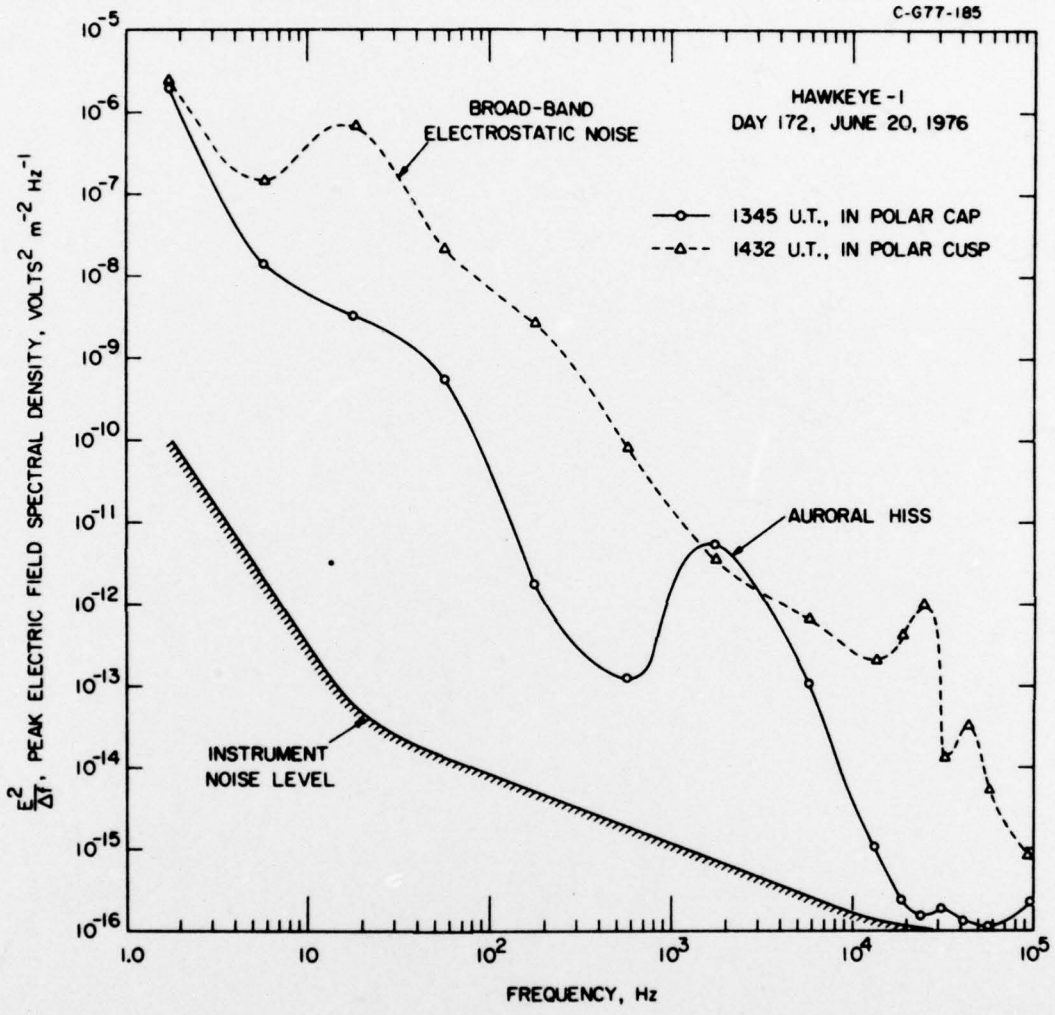
C-G77-185
HAWKEYE-I
DAY 172, JUNE 20, 1976
BROAD-BAND
ELECTROSTATIC NOISE
1345 U.T., IN POLAR CAP
1432 U.T., IN POLAR CUSP
AURORAL HISS
INSTRUMENT
NOISE LEVEL
$\frac{E^2}{\Delta f}$, PEAK ELECTRIC FIELD SPECTRAL DENSITY, VOLTS^2 m^{-2} Hz^{-1}
FREQUENCY, Hz

Figure 6

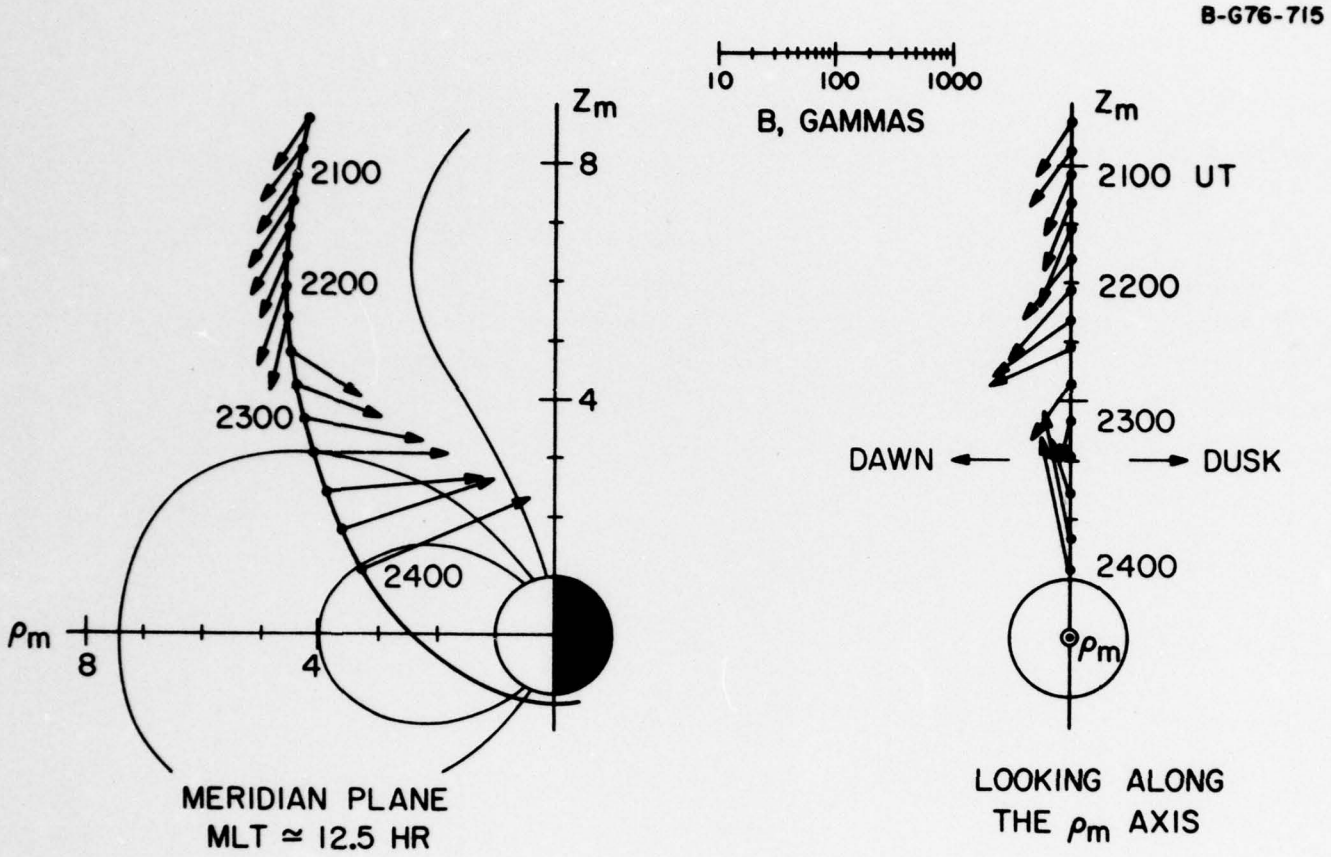

HAWKEYE-I, DAY 186, JULY 5, 1974

Figure 7

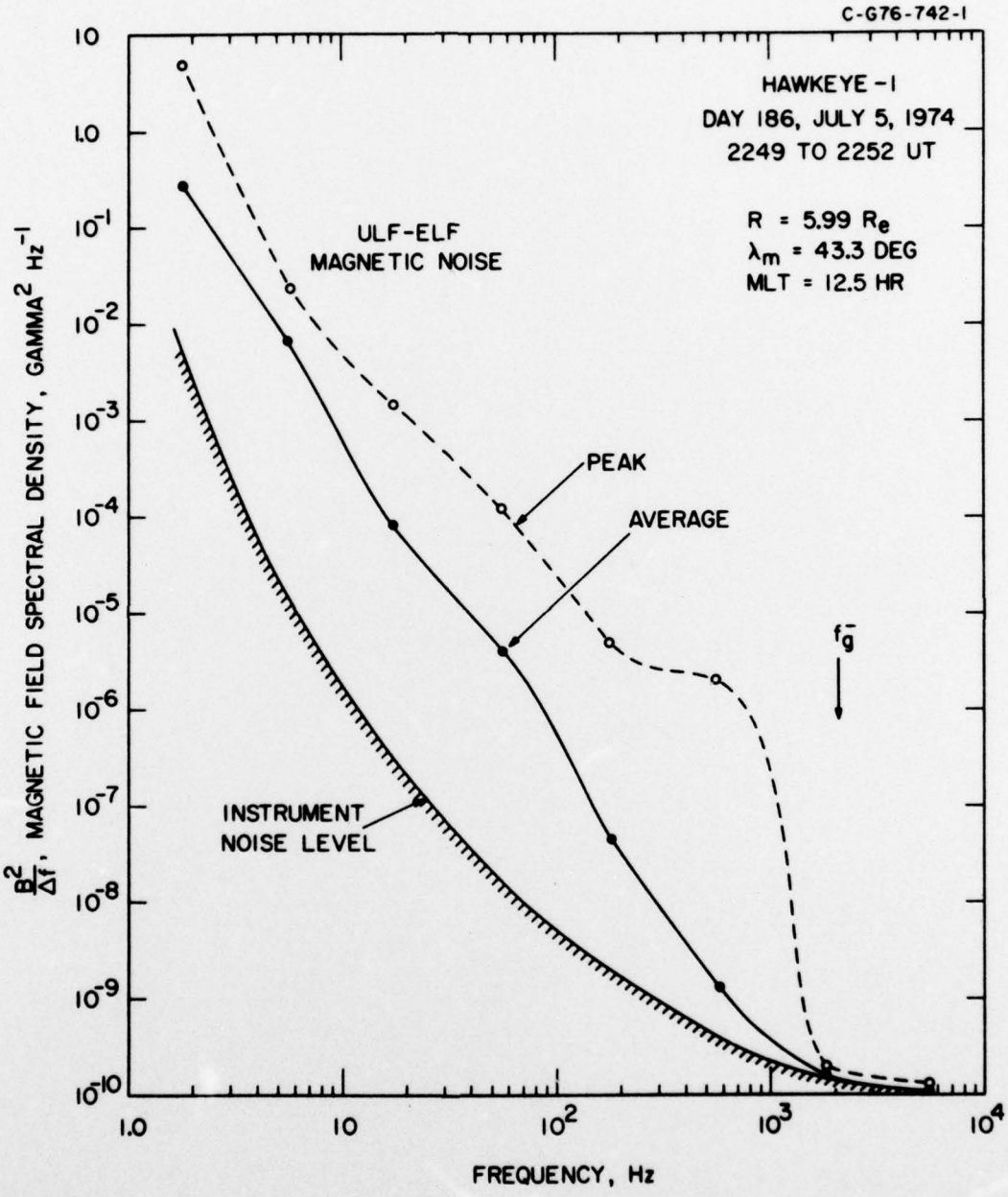
C-G76-742-1
HAWKEYE-1
DAY 186, JULY 5, 1974
2249 TO 2252 UT
R = 5.99 Re
λm = 43.3 DEG
MLT = 12.5 HR
ULF-ELF
MAGNETIC NOISE
PEAK
AVERAGE
fg
INSTRUMENT
NOISE LEVEL
B²/Δf, MAGNETIC FIELD SPECTRAL DENSITY, GAMMA² Hz⁻¹
FREQUENCY, Hz
10
1.0
10⁻¹
10⁻²
10⁻³
10⁻⁴
10⁻⁵
10⁻⁶
10⁻⁷
10⁻⁸
10⁻⁹
10⁻¹⁰
1.0
10
10²
10³
10⁴

Figure 8

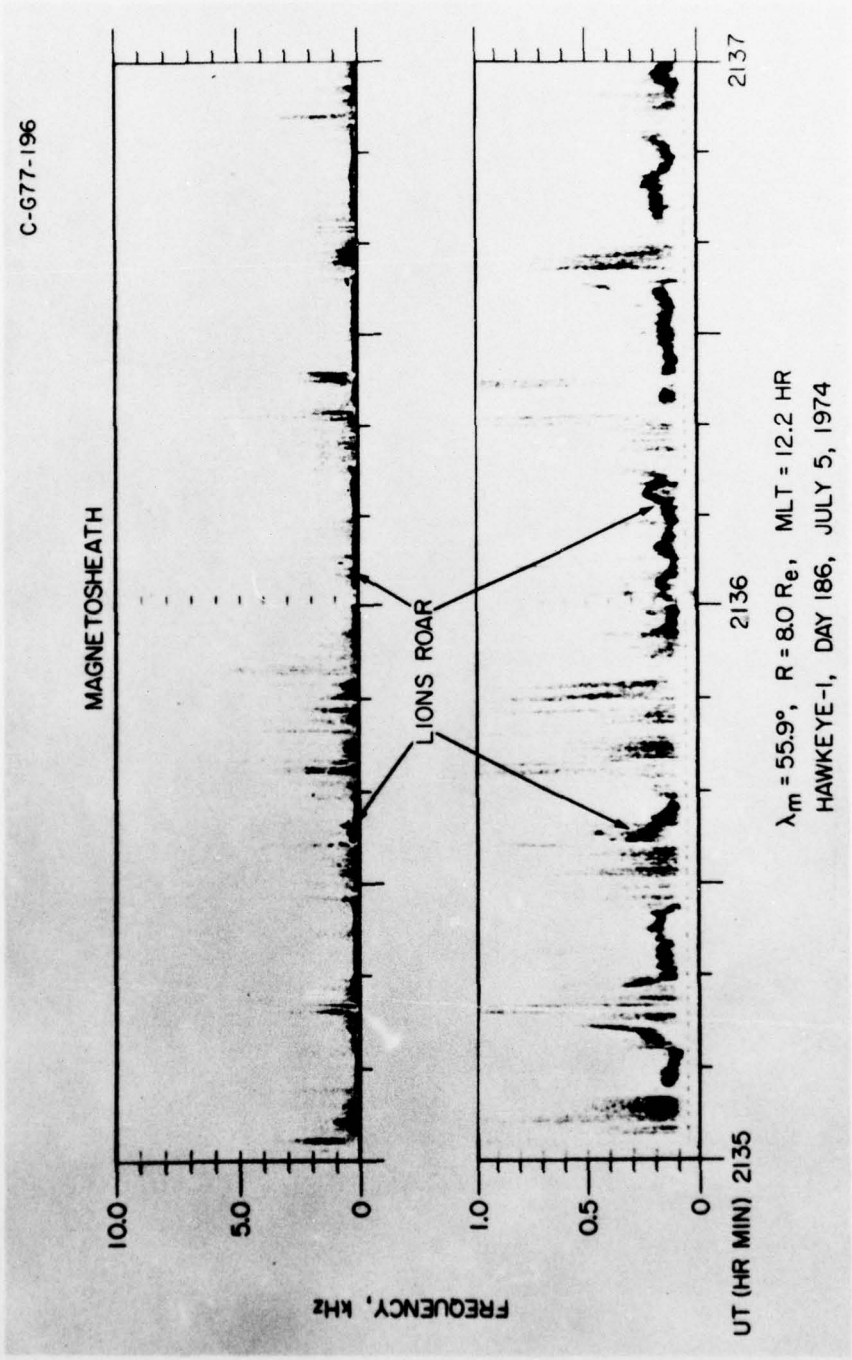
C-G77-196
MAGNETOSHEATH
LIONS ROAR
10.0
5.0
0
1.0
0.5
0
FREQUENCY, kHz
UT (HR MIN) 2135
2136
2137
λ_m = 55.9°, R = 8.0 R_e, MLT = 12.2 HR
HAWKEYE-1, DAY 186, JULY 5, 1974

Figure 9

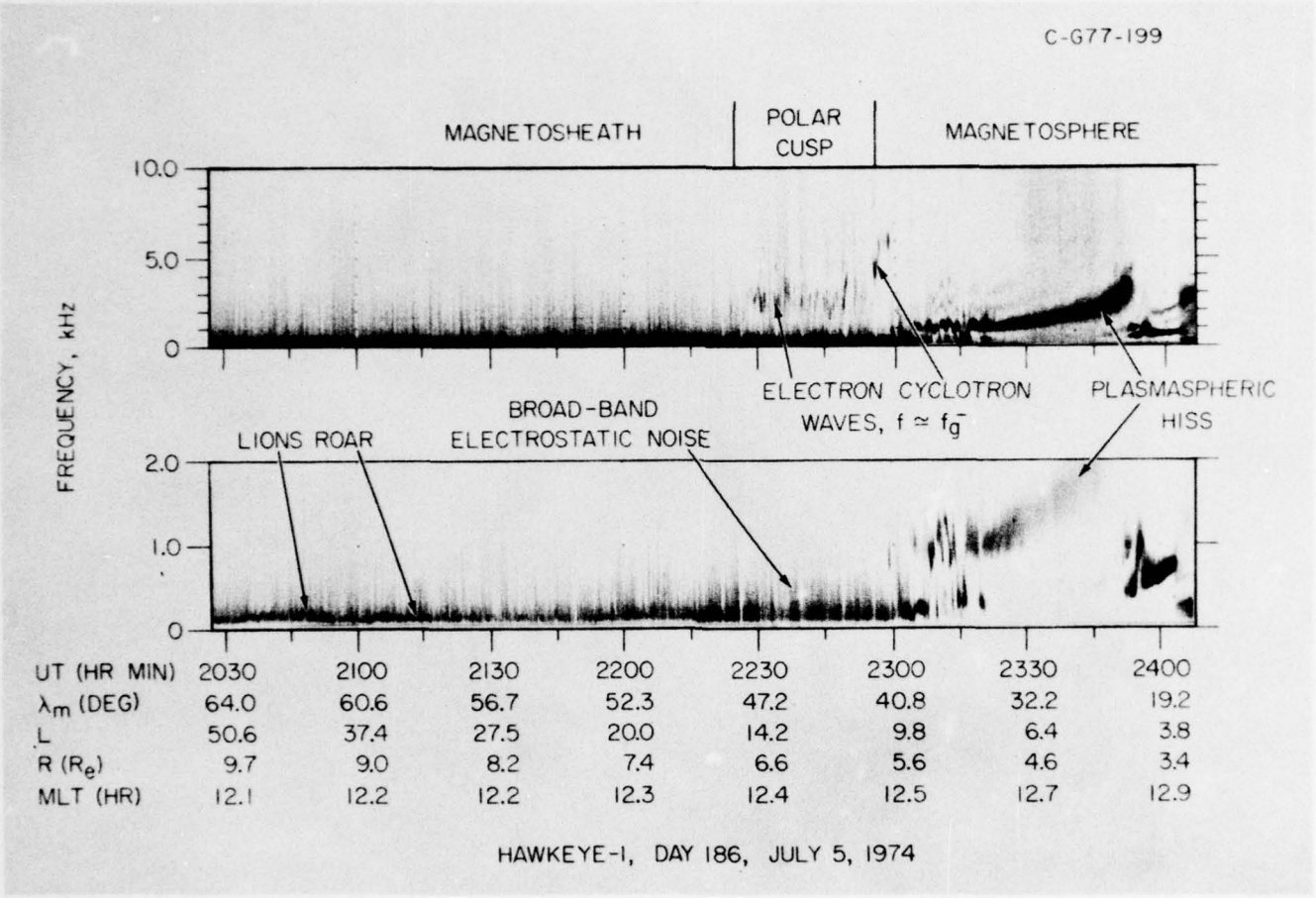
C-G77-199
MAGNETOSHEATH
POLAR CUSP
MAGNETOSPHERE
10.0
5.0
0
FREQUENCY, kHz
ELECTRON CYCLOTRON WAVES, f ≃ fg⁻
PLASMASPHERIC HISS
BROAD-BAND ELECTROSTATIC NOISE
LIONS ROAR
2.0
1.0
0
UT (HR MIN) 2030 2100 2130 2200 2230 2300 2330 2400
λm (DEG) 64.0 60.6 56.7 52.3 47.2 40.8 32.2 19.2
L 50.6 37.4 27.5 20.0 14.2 9.8 6.4 3.8
R (Re) 9.7 9.0 8.2 7.4 6.6 5.6 4.6 3.4
MLT (HR) 12.1 12.2 12.2 12.3 12.4 12.5 12.7 12.9
HAWKEYE-1, DAY 186, JULY 5, 1974

Figure 10

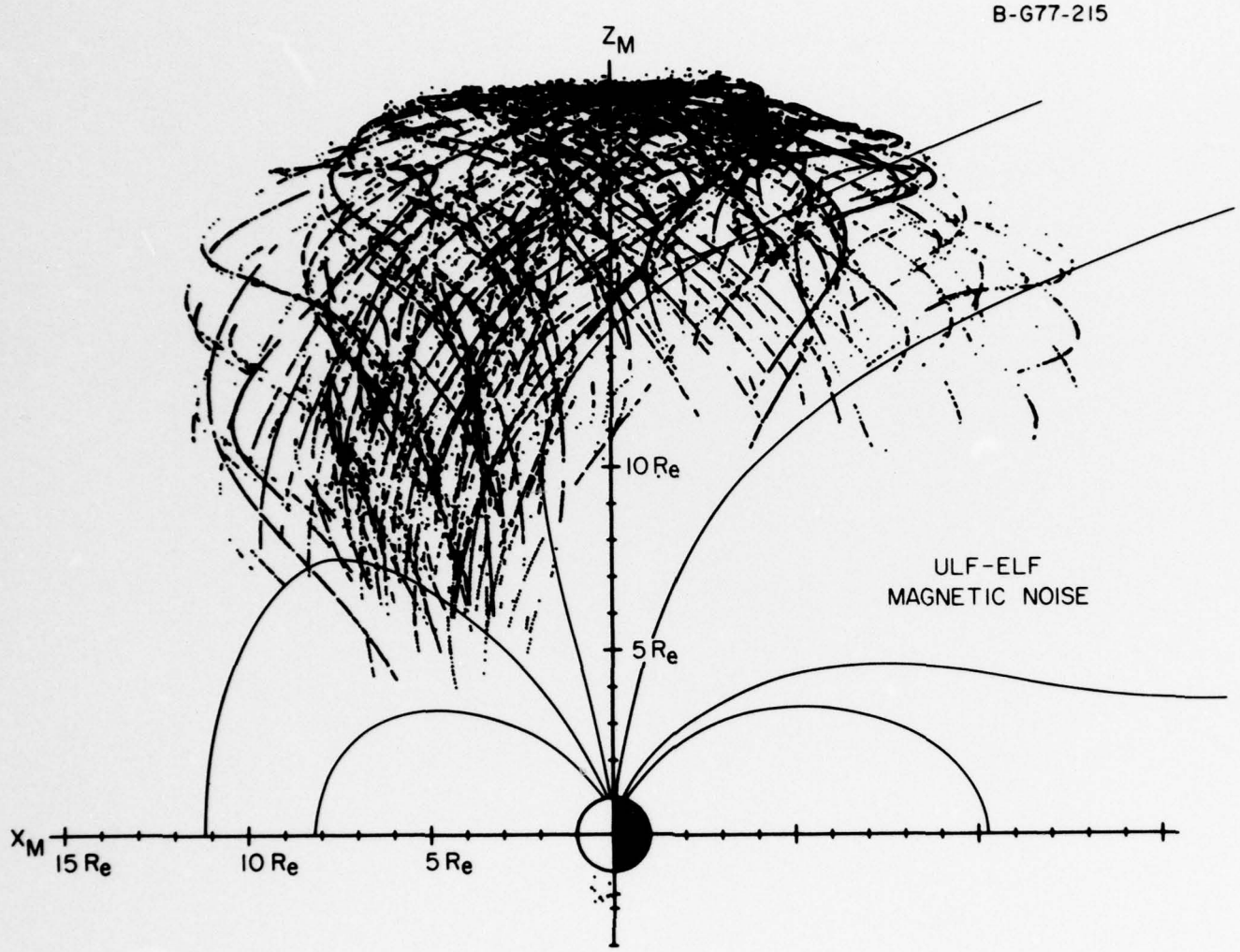

Figure 11

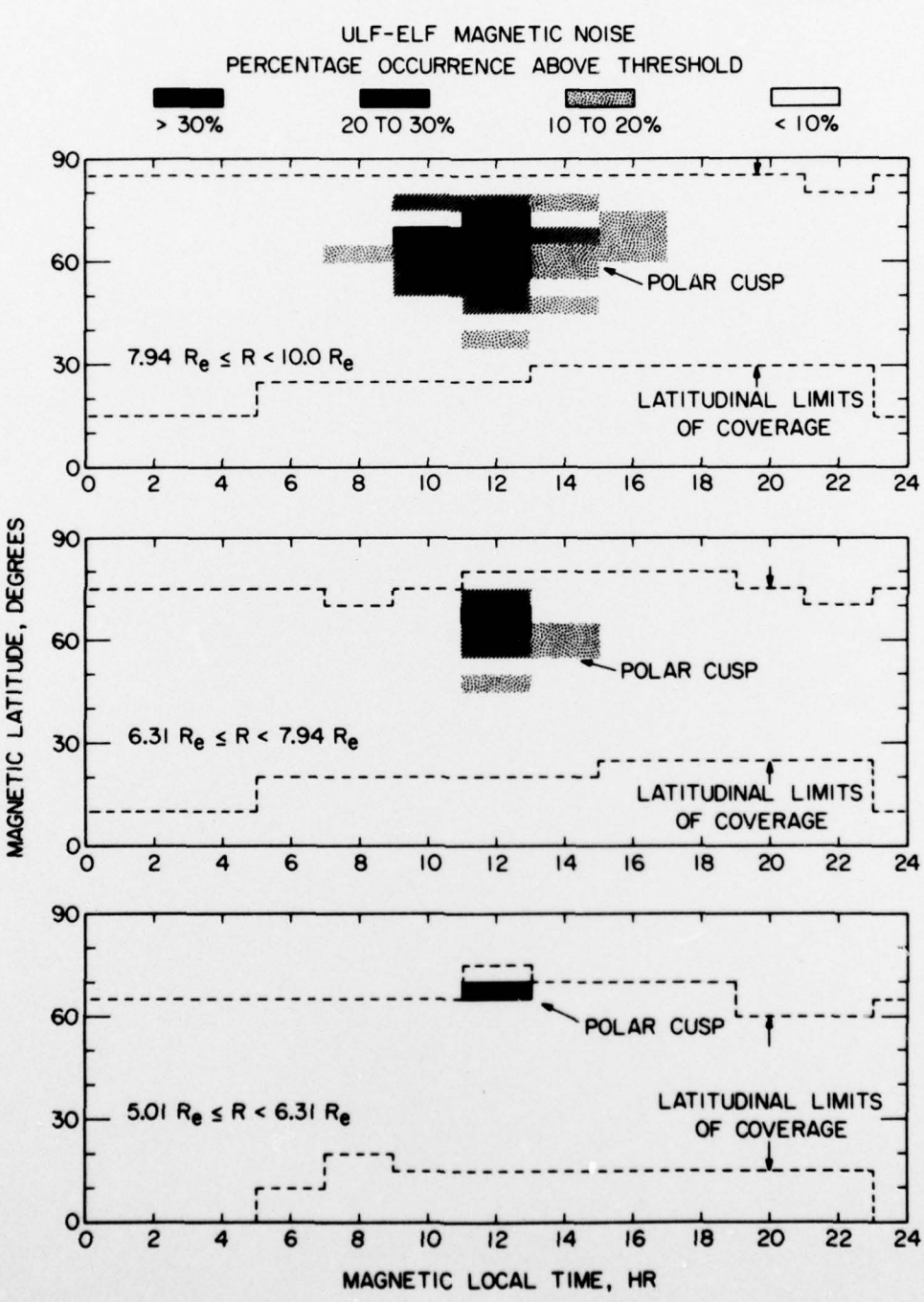
C-G77-191
ULF-ELF MAGNETIC NOISE
PERCENTAGE OCCURRENCE ABOVE THRESHOLD
> 30%
20 TO 30%
10 TO 20%
< 10%
POLAR CUSP
7.94 Re ≤ R < 10.0 Re
LATITUDINAL LIMITS OF COVERAGE
6.31 Re ≤ R < 7.94 Re
5.01 Re ≤ R < 6.31 Re
MAGNETIC LATITUDE, DEGREES
MAGNETIC LOCAL TIME, HR

Figure 12

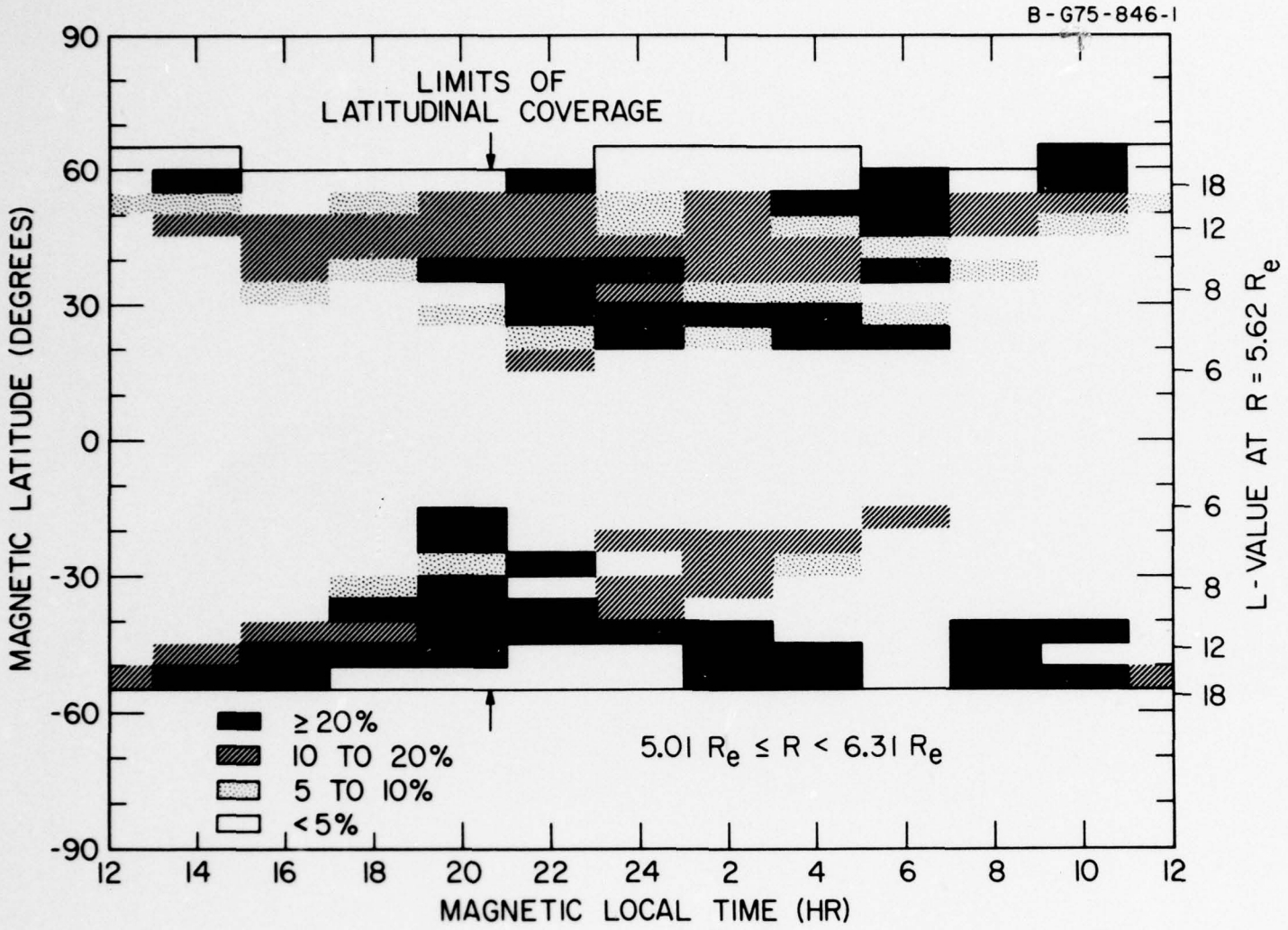
B-G75-846-1
LIMITS OF
LATITUDINAL COVERAGE
MAGNETIC LATITUDE (DEGREES)
90
60
30
0
-30
-60
-90
12
14
16
18
20
22
24
2
4
6
8
10
12
MAGNETIC LOCAL TIME (HR)
L-VALUE AT R = 5.62 Re
18
12
8
6
6
8
12
18
≥ 20%
10 TO 20%
5 TO 10%
< 5%
5.01 Re ≤ R < 6.31 Re

Figure 13

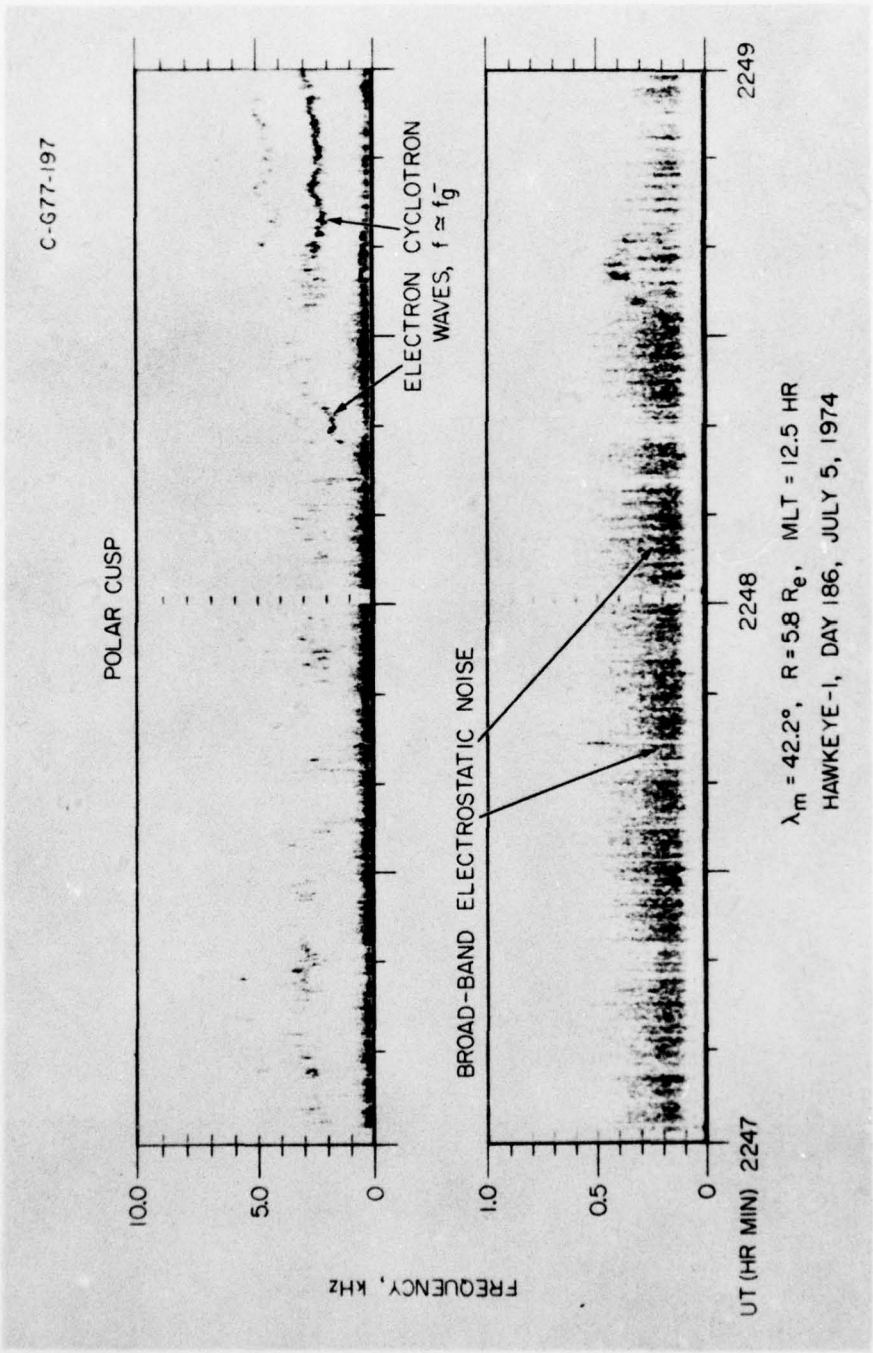
C-G77-197
POLAR CUSP
ELECTRON CYCLOTRON WAVES, $f \simeq f_g$
BROAD-BAND ELECTROSTATIC NOISE
FREQUENCY, kHz
10.0
5.0
0
1.0
0.5
0
UT (HR MIN) 2247
2248
2249
λ_m = 42.2°, R = 5.8 R_e, MLT = 12.5 HR
HAWKEYE-1, DAY 186, JULY 5, 1974

Figure 14

C-G77-230

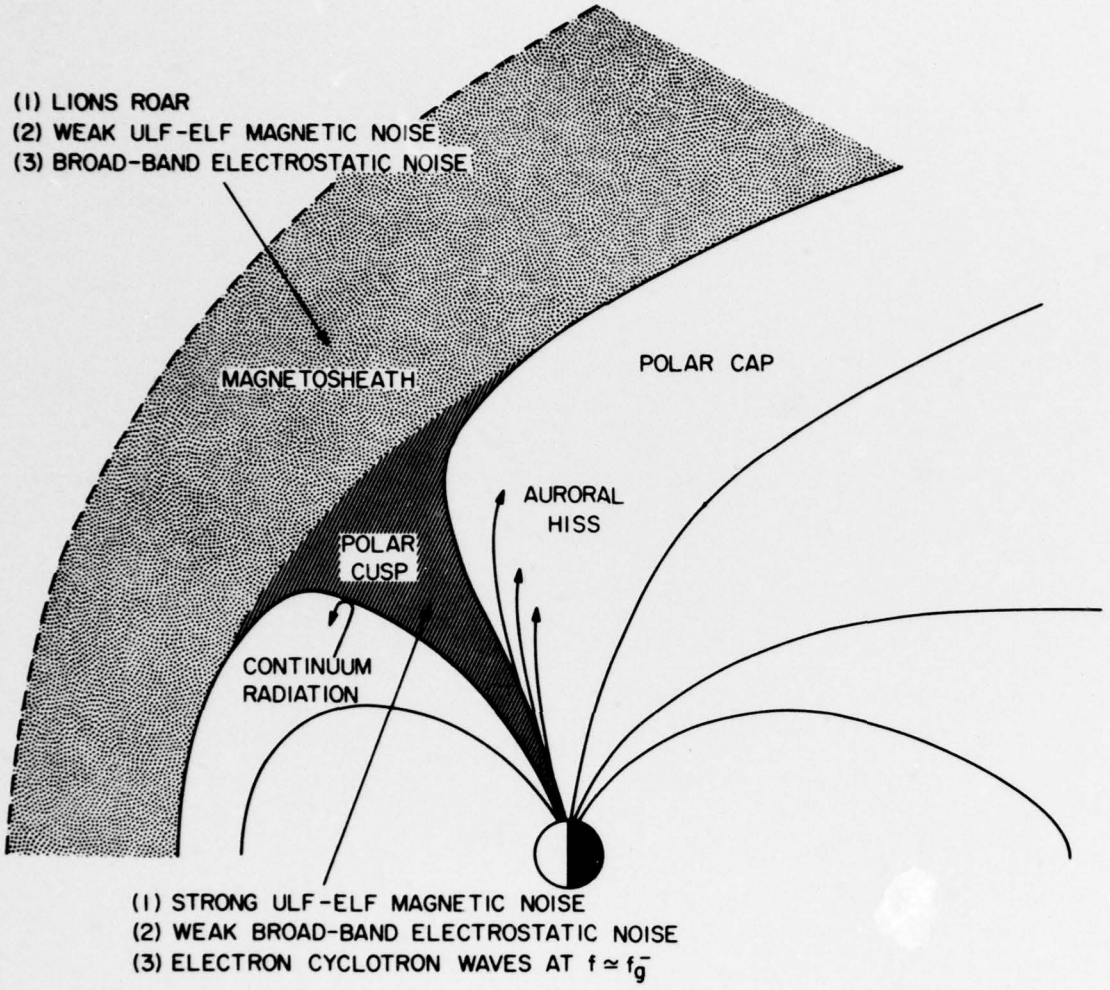

Figure 15

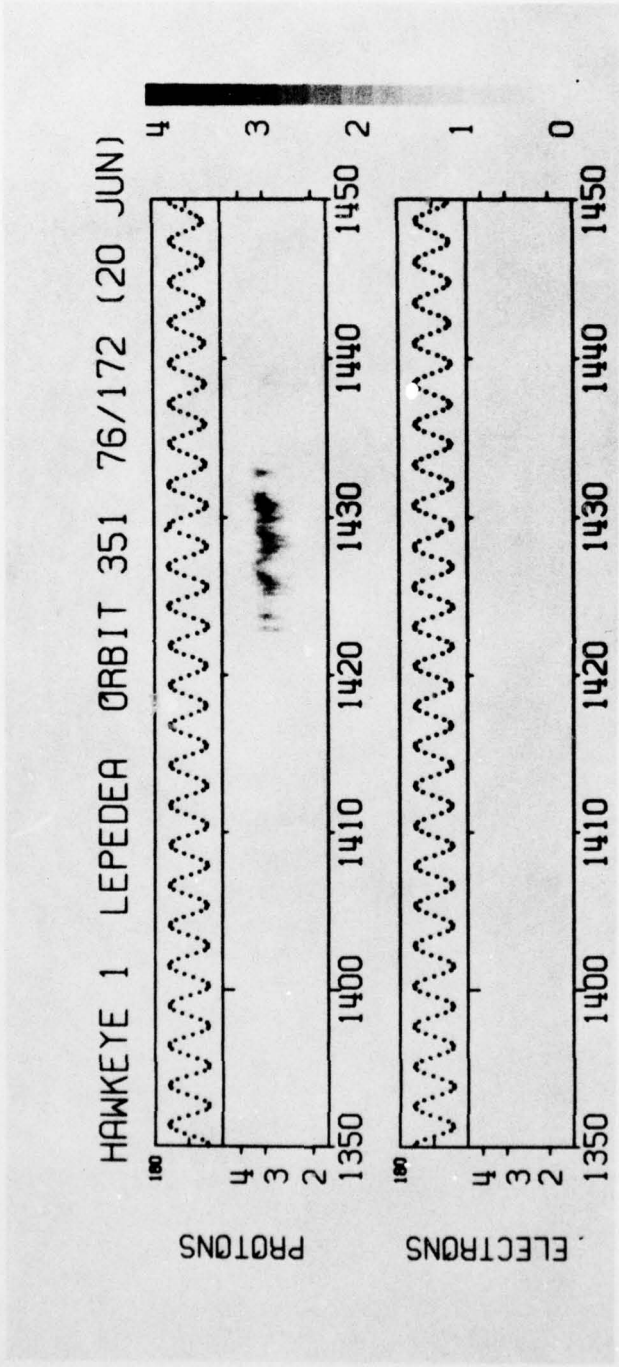
HAWKEYE 1 LEPEDEA ORBIT 351 76/172 (20 JUN)
PROTONS
ELECTRONS
180
4
3
2
1350
1400
1410
1420
1430
1440
1450
1
0

Plate 1

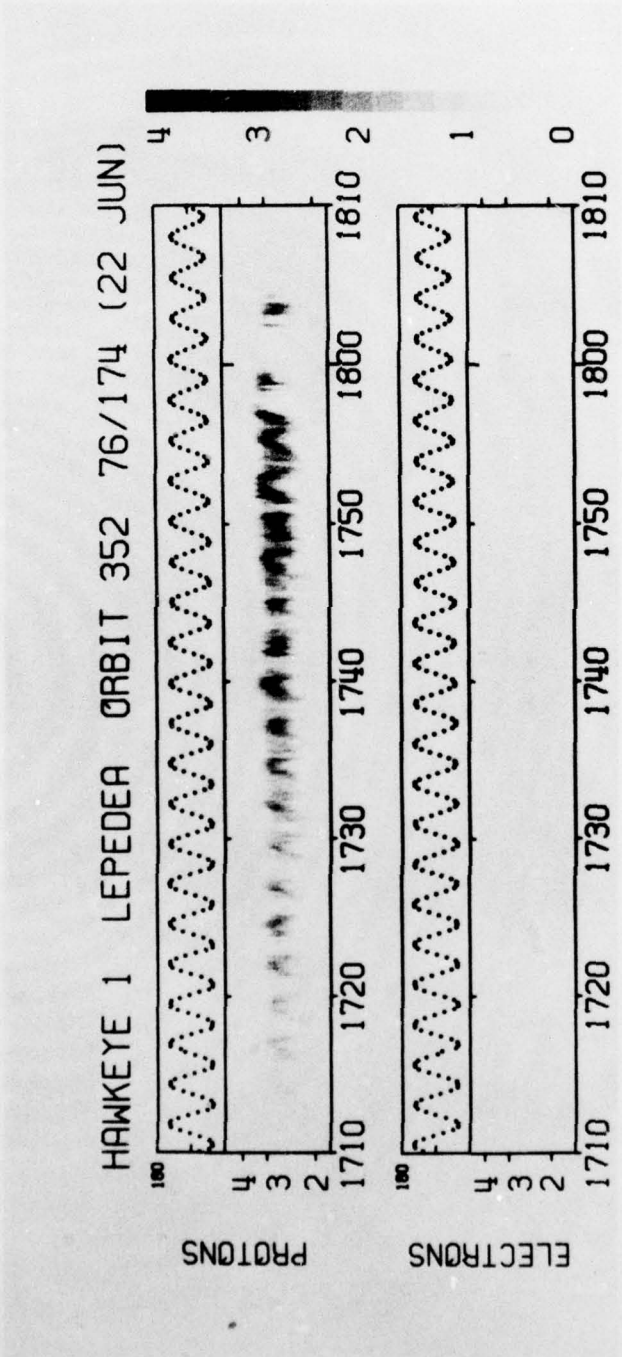
HAWKEYE 1 LEPEDEA ORBIT 352 76/174 (22 JUN)
PROTONS
ELECTRONS
180
4
3
2
1710
1720
1730
1740
1750
1800
1810
1
0

Plate 2

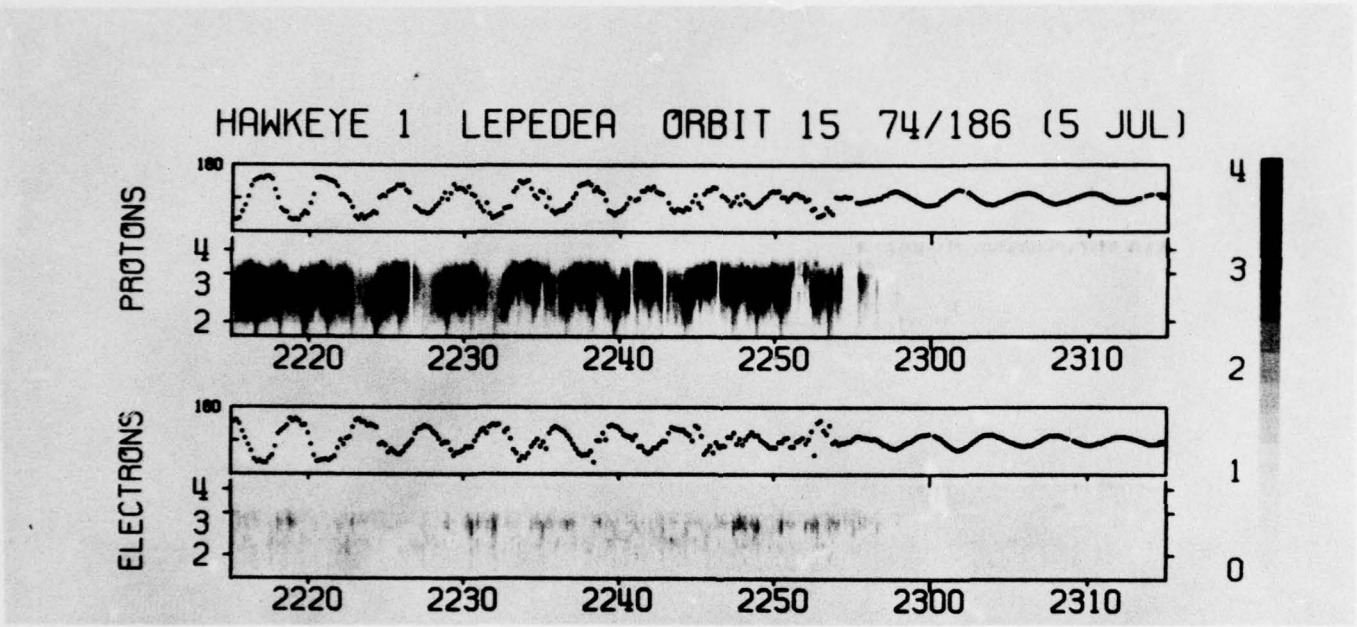
HAWKEYE 1 LEPEDEA ORBIT 15 74/186 (5 JUL)
PROTONS
ELECTRONS
180
4
3
2
2220
2230
2240
2250
2300
2310
4
3
2
1
0

Plate 3

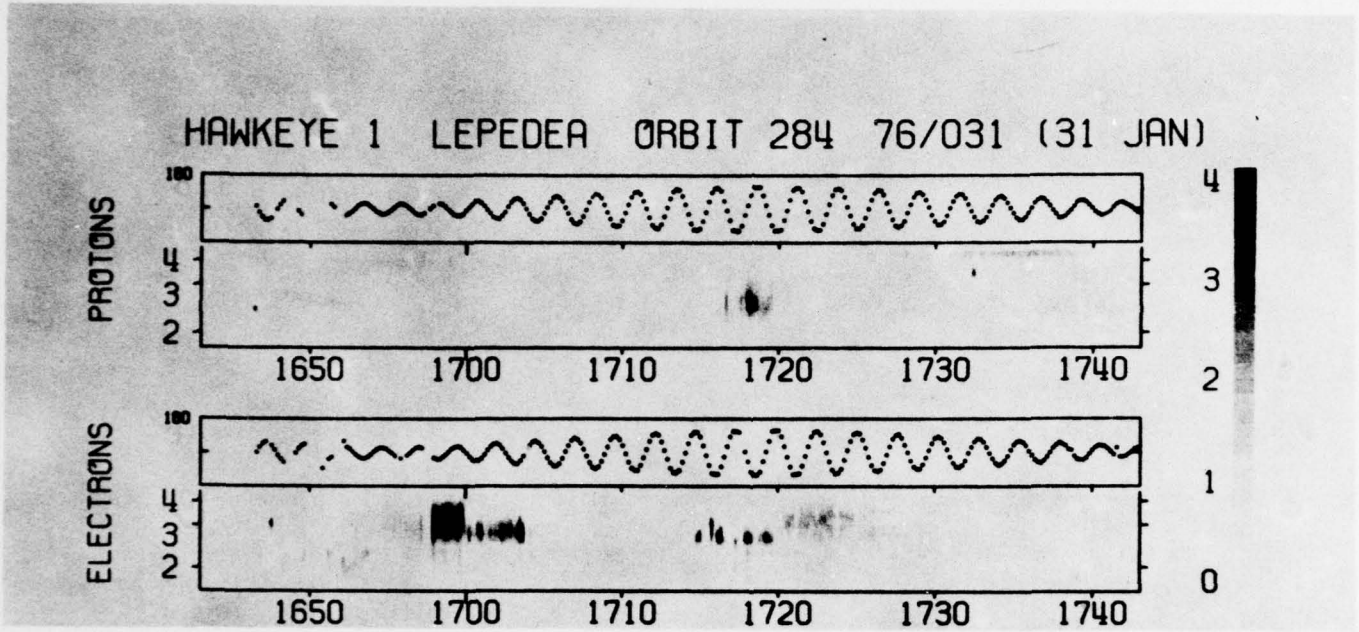
HAWKEYE 1 LEPEDEA ORBIT 284 76/031 (31 JAN)
PROTONS
ELECTRONS
180
4
3
2
1650
1700
1710
1720
1730
1740
4
3
2
1
0

Plate 4